Naval Research Laboratory
Washington, DC 20375-5320

Rechargeable Zn-Air Batteries with Pulse-Power Capability

Christopher N. Chervin
Jeffrey W. Long
Joseph F. Parker
Debra R. Rolison

Surface Chemistry Branch
Chemistry Division

June 8, 2020

REPORT DOCUMENTATION PAGE

1. REPORT DATE (DD-MM-YYYY) 08-06-2020	2. REPORT TYPE NRL Memorandum Report	3. DATES COVERED (From - To) 1 Oct 16 – 30 Sept 19

4. TITLE AND SUBTITLE

Rechargeable Zn-Air Batteries with Pulse-Power Capability

5a. CONTRACT NUMBER

5b. GRANT NUMBER

5c. PROGRAM ELEMENT NUMBER
62123N

6. AUTHOR(S)

Christopher N. Chervin, Jeffrey W. Long, Joseph F. Parker, and Debra R. Rolison

5d. PROJECT NUMBER

5e. TASK NUMBER

5f. WORK UNIT NUMBER
6A01

7. PERFORMING ORGANIZATION NAME(S) AND ADDRESS(ES)

Naval Research Laboratory
4555 Overlook Avenue, SW
Washington, DC 20375-5320

8. PERFORMING ORGANIZATION REPORT NUMBER

NRL/MR/6171--20-10,033

9. SPONSORING / MONITORING AGENCY NAME(S) AND ADDRESS(ES)

10. SPONSOR / MONITOR'S ACRONYM(S)

11. SPONSOR / MONITOR'S REPORT NUMBER(S)

12. DISTRIBUTION / AVAILABILITY STATEMENT

DISTRIBUTION STATEMENT A: Approved for public release distribution is unlimited.

13. SUPPLEMENTARY NOTES

14. ABSTRACT

See report Title Page.

15. SUBJECT TERMS

16. SECURITY CLASSIFICATION OF:			17. LIMITATION OF ABSTRACT	18. NUMBER OF PAGES	19a. NAME OF RESPONSIBLE PERSON Christopher N. Chervin
a. REPORT Unclassified Unlimited	**b. ABSTRACT** Unclassified Unlimited	**c. THIS PAGE** Unclassified Unlimited	Unclassified Unlimited	42	**19b. TELEPHONE NUMBER** (include area code) (202) 404-1593

This page intentionally left blank.

RECHARGEABLE ZN–AIR BATTERIES WITH PULSE-POWER CAPABILITY

Christopher N. Chervin, Jeffrey W. Long, Joseph F. Parker, and Debra R. Rolison
Code 6170, Surface Chemistry Branch
Naval Research Laboratory
4555 Overlook Avenue, Washington, DC 20375

ABSTRACT

Zinc–air batteries are energy-storage devices that are safe to operate (thanks to nonflammable aqueous electrolytes), use an abundant, domestically sourced active material (Zn), and provide high specific energy by harvesting O_2 from air to serve as the oxidant. Despite these attractive features, the implementation of Zn–air batteries for military and civilian applications is constrained by the limited rechargeability and power response of present Zn–air technology. The Advanced Electrochemical Materials Section at the U.S. Naval Research Laboratory executed a 6.2 research program from FY16–FY19 in which the focus was to address remaining roadblocks to high-performance, rechargeable Zn–air batteries through targeted development efforts and leveraging related developments at the NRL with advanced 3D porous Zn electrodes. The core of this program was the development of a trifunctional air cathode—the first of its kind—that expresses the three critical functions of O_2-evolution reaction (OER), O_2-reduction reaction (ORR), and pulse-power. The trifunctional cathode comprises a powder composite layer functionalized with pre-formed OER and ORR catalysts that are bonded to a MnO_x-modified carbon nanofoam paper that provides pulse-power. En route to the final cathode structure, bifunctional (ORR + OER) catalysts were designed, fabricated, and their electrochemical performance and stability were optimized. Down-selected bifunctional air cathodes were paired with the NRL-patented Zn sponge anode in prototype coin cells to demonstrate Zn–air cell performance and rechargeability. The combination of the bifunctional composite cathode with pulse-power enabling MnO_x-modfied carbon nanofoams was then demonstrated. The advances derived from this 6.2 program readily transition to civilian and military uses, and serve as an enabling technology for the portable-power requirements of the next-generation warfighter.
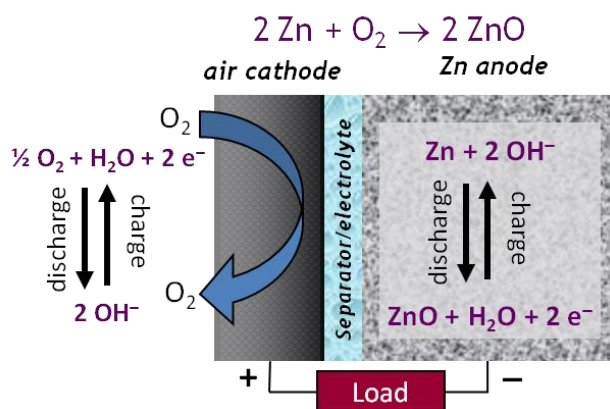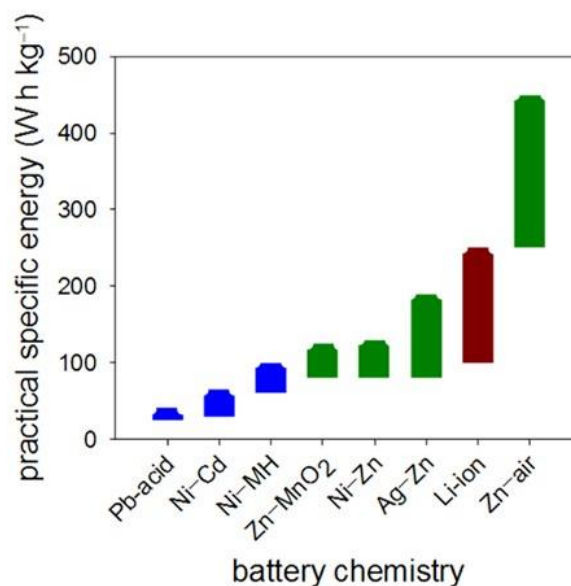
BACKGROUND

The increasing demand for safe, high-energy density power sources to support a wide range of DoD applications, including portable power for the warfighter and on-board power for unmanned vehicles, highlights a critical need for advanced battery technologies. While lithium-ion (Li-ion) batteries offer substantial benefits for these applications (e.g., reasonable energy density, rechargeability, and commercial availability), their use for the military is severely limited by an unacceptable safety track-record.[1] A fireproof battery alternative, zinc–air, has high practical specific

Figure 1. Practical specific energy densities for a variety of battery chemistries.

energy density >400 W h kg^{-1} (almost double that of Li-ion; see Figure 1) and the advantage of a cheap and environmentally friendly active material (zinc; Zn) coupled to cathodes that consume molecular oxygen supplied directly from ambient air (Figure 2).[2] While successful as a primary (single use) battery in specific commercial applications (e.g., the hearing-aid market) and military uses (one-time recharge of Li-ion), the broader implementation of Zn–air battery technology has been historically hindered by poor rechargeability and moderate power output. These limitations can be ascribed to multiple factors inherent to conventional forms of both the Zn anode and the air-breathing cathode.

In order to direct our research and development efforts, we identified four key functionalities that must be exhibited by successful rechargeable Zn–air batteries, as shown in Figure 3: (*i*) "battery" behavior at the Zn anode, as manifested by dendrite-free

Figure 2. Schematic of a rechargeable Zn–air battery.

[1] Lee, J.-S.; Kim, S. T.; Cao, R.; Choi, N.-S.; Liu, M.; Lee, K. T.; Cho, J. *Adv. Energy Mater.* **2011**, *1*, 34–50.
[2] Neburchilov, V.; Wang, H.; Martin, J. J.; Qu, W. *J. Power Sources* **2010**, *195*, 1271–1291.

cycling at high depth-of-discharge; (*ii*) "fuel cell" functionality, where reduction of O_2 (from air) is efficiently catalyzed in the cathode during discharge; (*iii*) "electrolyzer" operation, where the ORR reaction is reversed to generate O_2 upon cell recharge; and (*iv*) "electrochemical capacitor" functionality to support momentary pulse-power at rates not available with ORR alone.
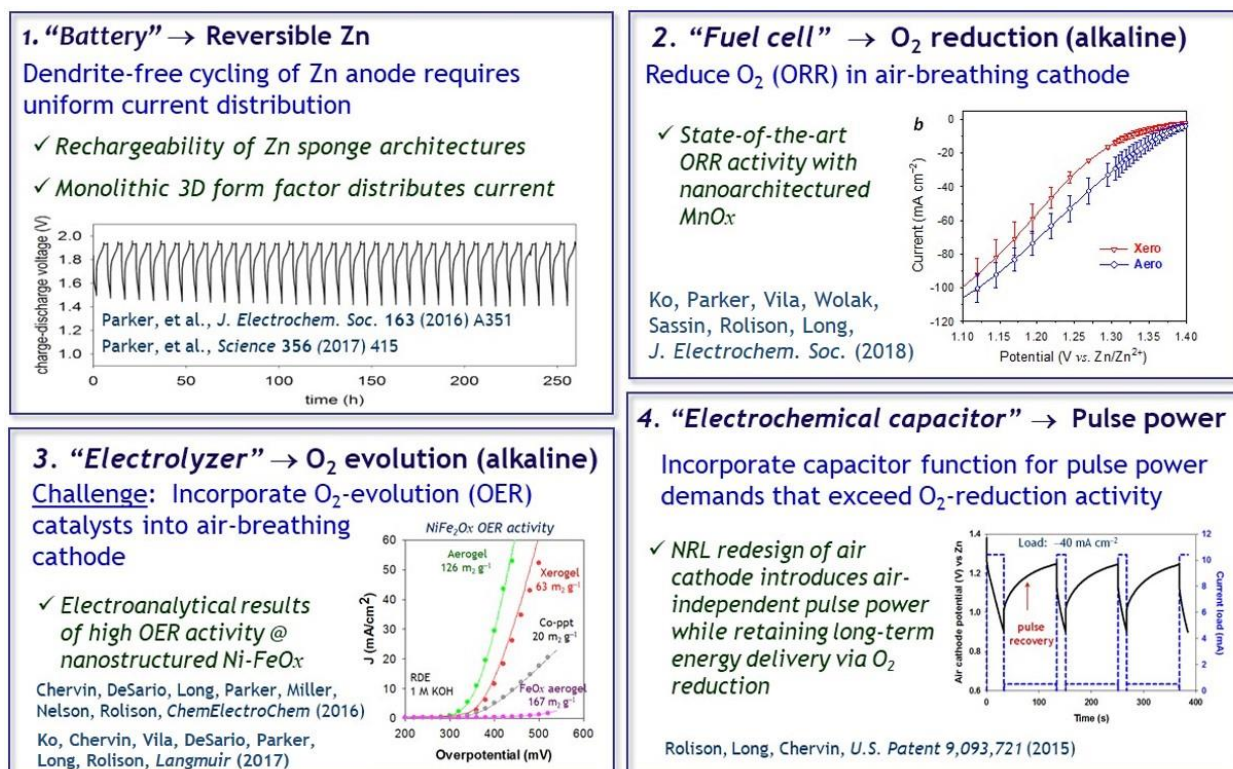
Figure 3. The four critical functions that will enable rechargeable Zn–air batteries as a safe alternative to Li-ion batteries.

All alkaline zinc batteries historically have been limited in terms of rechargeability due to the propensity of zinc electrodes to generate short circuit–inducing dendrites and to undergo shape change during extended charge–discharge cycling, particularly when using standard powder-composite negative electrodes comprising zinc powder mixed with gelling agents, electrolyte, and/or binders. We recently demonstrated a solution to this localized, anomalous dendrite-forming problem by fabricating the Zn anode as a pore–solid architecture in which the 3D-interconnected pore volume is co-continuous with the 3D-interconnected solid zinc network,

i.e., a "sponge."[3,4] The fully metallic, conductive pathways in 3D improve current distribution throughout the electrode structure and avoid uneven reaction loci where formation of dendrites is likely to occur during charge–discharge cycles.[1,5] In addition, the pore network intertwined throughout the 3D zinc scaffold helps to constrain the soluble discharge products and promote rapid precipitation of the final discharge product, ZnO, at nearby Zn surfaces, thereby further minimizing electrode shape change and cross-over of Zn species to the cathode. By fabricating the Zn anode in a 3D porous form factor (sponge morphology), we achieve 90% Zn utilization (with respect to theoretical capacity) in a primary Zn–air cell and dendrite-free cycling in secondary Ag–Zn and Ni–Zn cells.

A long-standing challenge for rechargeable Zn–air batteries is the development of a multi-functional air cathode that can simultaneously facilitate three critical functions: oxygen reduction reaction (ORR) for battery discharge; oxygen evolution reaction (OER) for battery recharge; and a mechanism to provide pulse-power beyond the limitations of ORR kinetics. To achieve these functions, the physical structure of the air cathode must support $O_2(g)$ transport, ion transport, and electrocatalytic reactivity—properties that are achieved using "brick-and-mortar" methods to form a powder composite comprising carbon black, catalyst particles, and a hydrophobic polymeric binder. Although functional, the ad-hoc distribution of voids within the volume of the typical composite air cathode adversely affects $O_2(g)$ flux and limits the specific power of the metal–air battery. We have addressed the power limitations of air cathodes by applying an architectural perspective to a redesign of the air cathode, using fiber-supported carbon nanofoam papers as the base electrode platform.[6,7] Electrocatalytic ORR functionality is imparted to the carbon nanofoam by incorporating conformal, nanoscale birnessite-like MnO_x coatings (10–20-nm thick) using a simple electroless deposition procedure.[8] Additionally, the nanoscale, conformal MnO_x coating imparts pulse-power functionality to the air cathode allowing for

[3] Parker, J. F.; Nelson, E. S.; Wattendorf, M. D.; Chervin, C. N.; Long, J. W.; Rolison, D. R. *ACS Appl. Mater. Interfaces* **2014**, *6*, 19471–19476.

[4] Parker, J. F.; Chervin, C. N.; Nelson, E. S.; Rolison, D. R.; Long, J. W. *Energ. Environ. Sci.* **2014,** *7*, 1117–1124.

[5] Arora, P.; Zhang, Z. *Chem. Rev.* **2004**, *104*, 4419–4462.

[6] Chervin, C. N.; Long, J. W.; Brandell, N. L.; Wallace, J. M.; Kucko, N. W.; Rolison, D. R. *J. Power Sources* **2012**, *207*, 191–199.

[7] Long, J. W.; Chervin, C. N.; Kucko, N. W.; Nelson, E. S.; Rolison, D. R. *Adv. Energy Mater.* **2013**, *3*, 584–588. [*2013 6.2 Berman Award winner*]

[8] Sassin, M.B.; Long, J.W.; Chervin, C.N.; Rolison, D.R. *Acc. Chem. Res.* **2013**, *46*, 1062 –1074.

air-independent current pulses (>100 mA cm^{-2}) for several seconds,[7] courtesy of MnOx pseudocapacitance (Figure 3, bottom right).
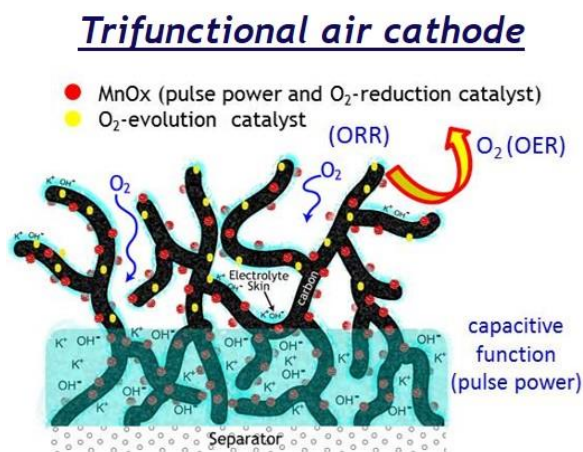
The early development breakthroughs noted above for both Zn anodes and multifunctional air cathodes motivated our proposal and execution of the present 6.2 program, whose further advances are described in this report.

TECHNICAL OBJECTIVE

This program's objective was to leverage the established performance of NRL's Zn sponge anode to pair with new air cathode designs to demonstrate a new class of safe, high-performance, rechargeable Zn–air batteries for future military and civilian applications. A key challenge for the cathode redesign is to incorporate recharge-enabling OER catalysts while maintaining the pulse-power function of the MnOx-modified carbon nanofoam such that the resulting air cathode is "trifunctional", supporting ORR, OER, and pulse power (see Figure 4). An additional challenge to this program was the design, assembly, and testing of prototype rechargeable Zn–air cells with respect to parameters including electrolyte and separator choice, cycling conditions, electrolyte management, and cell sealing. The development of rechargeable Zn–air batteries with pulse-power capabilities is critical for the Navy and DoD, offering the opportunity to displace hazardous Li-ion batteries for applications ranging from portable power for the soldier/marine to defense systems and electric vehicles. Advances derived from this 6.2 program serve as enabling technology for low-cost, safe-to-operate portable-power requirements of the next-generation warfighter.

Figure 4. A proposed schematic of a trifunctional air cathode comprising a capacitive-function layer married to a gas-diffusion catalyst layer functionalized with ORR and OER electrocatalysts

TECHNICAL APPROACH

At the onset of this program, we set forth to develop methods to fabricate the proposed trifunctional cathode and complete the following key tasks:

Oxygen-evolution functionality: Demonstrate OER and bifunctional OER/ORR activity of NRL-developed nanostructured iron oxides (e.g., M-FeOx; M = V, Ni, Cu, Zr, or Ti) using standard electroanalytical techniques and benchmark against known oxidation catalysts for alkaline electrolytes, such as NiOx and perovskites (e.g., La$_{1-x}$Ca$_x$CoO$_3$). The most active catalysts would then be incorporated within the proposed cathode architecture.

Catalyst optimization within air cathodes: Optimize the composition, distribution, and loading of electrocatalyst (e.g., Orr AT MnOx plus OER at M-FeOx) within the proposed cathode architecture to maximize ORR, OER, and pulse-power activity, as established using Code 6171-designed electroanalytical protocols. Use down-selected cathodes in air-breathing electroanalytical cells; test for such performance metrics as current density of ORR and OER at practical Zn–air cell voltages and pulse-power response in the face of challenging duty-cycle conditions.

Full-cell fabrication and testing: Integrate down-selected cathode architectures and Zn sponge anodes into Zn–air full cells and evaluate performance in primary and rechargeable mode with respect to the following parameters:

 (i) Minimizing OER overpotential to decrease charge–discharge voltage hysteresis. Demonstrate that down-selected OER catalysts are capable of supporting a charge–discharge hysteresis of <800 mV at a technologically relevant current load (10 mA cm^{-2});

 (ii) Long-term cycling stability. Monitor for possible cross-contamination, such as carbonaceous deposits on the Zn anode and insoluble Zn species on the air cathode, through post-mortem characterization (e.g., ex-situ Raman, SEM, XPS, and XRD) after extensive cycling in Zn–air cells. Demonstrate that insoluble carbonate byproducts (formed by contamination from atmospheric CO$_2$) can be successfully mitigated at the air cathode architecture by pH swings accompanying electrochemical processes during recharge or by using CO$_2$-rejecting/O$_2$-permeable membranes;

 (iii) Impact of load on cell capacity and discharge voltage under both constant-current draw (5–100 mA cm^{-2}) and complex duty cycles. Demonstrate pulse-power performance of Zn–air full cells with a duty cycle of moderate load (10 mA cm^{-2}) interspersed by tens-of-seconds high

pulse-power draws (up to 150 mA cm^{-2}); pulses will approximate specific power of 700 W kg^{-1} normalized to the Zn mass.

EXPERIMENTS

1. Electrocatalyst design for air cathodes

A major challenge for rechargeable Zn–air batteries is the identification of a stable and efficient air-breathing positive electrode that incorporates high-performance electrocatalysts to promote both oxygen reduction on discharge and oxygen evolution on recharge (Equation 1 and 2). The gas-diffusion cathode must also support facile flux of molecular oxygen to and from the catalytic sites, maintain electrolyte infiltration without flooding of the porous structure, and retain electronic conductivity throughout the electrode to promote relatively high discharge and charge rates. These requirements demand a multifunctional architecture designed to optimize catalysis, electrolyte management, and electrode and catalyst stability.

$$O_2 + 2H_2O + 4e^- \rightarrow 4OH^-; \textbf{ ORR} \tag{1}$$

$$4OH^- \rightarrow O_2 + 2H_2O + 4e^-; \textbf{ OER} \tag{2}$$

This pairing of ORR and OER catalysts within one gas-diffusion electrode is achieved either with two distinct electrocatalysts or with a single bifunctional catalyst that supports both reactions at technologically relevant rates and cell voltages. The benefit gained from distinct ORR and OER catalysts is increased flexibility to tune electrocatalytic activity for the individual reactions. However, this flexibility comes at the cost of greater electrode complexity and potential instability of the catalysts, particularly the ORR catalyst, which may oxidize under the corrosive conditions characteristic of OER. Integrating separate ORR and OER catalysts will also reduce the distribution of sites for each specific catalytic function on the electrode. Alternatively, incorporating a single bifunctional catalyst can solve these problems, but is challenging in practice because the respective mechanism for ORR and OER may not utilize the same active sites or reaction pathways and most materials only catalyze one reaction efficiently.

1A. Morphology as a tool to increase OER catalytic function[9]

The complex four-electron O_2-evolution reaction is associated with slow electrode kinetics that require the Zn–air battery to charge at a high oxidizing overpotential[10] to achieve technologically relevant rates (10 mA cm^{-2}). The high overpotential reduces device efficiency and contributes to oxidative corrosion of the air cathode components (e.g., carbon and catalysts).[11,12] Identifying inexpensive electrocatalysts that can minimize the overpotential for OER in alkaline electrolytes has led researchers beyond state-of-the-art noble metals (Pt, Ru, and Ir) to first-row transition-metal oxides,[13,14] including a range of nickel-ion spinels, layered double hydroxides, and oxyhydroxides.[13,15,16,17,18] Because of the higher cost of Ni and its known toxicity, establishing high OER activity with Fe-rich analogues is desirable for metal–air batteries. In this program, we leveraged our experience with Ni-substituted inverse spinel ferrites ($Ni_yFe_{1-y}Ox$, where the Ni:Fe stoichiometry is ≥ 1) to demonstrate the importance of pore-solid architecture when designing catalysts. We chose ferrite spinels because previous work identified them as promising OER catalysts, showing less than 400 mV overpotential at 10 mA cm^{-2}—a widely used performance metric for OER activity.[13,14,16]

We demonstrated that a single-phase, Fe-rich $NiFe_2Ox$ catalyst, once prepared as a porous nanoarchitecutre, achieves OER catalytic activity commensurate with Ni-rich compositions previously reported.[9,13] We did so by tuning the surface area and crystallinity of the oxide using aerogel synthesis techniques that produce much higher surface areas than are otherwise obtainable by conventional protocols. The $NiFe_2Ox$ nanoarchitectures were prepared via a versatile epoxide-initiated sol–gel method followed by either super critical drying with CO_2 to form aerogels or by ambient drying to form xerogels (Figure 5). To complete the morphological series,

[9] Chervin, C. N.; DeSario, P. A.; Parker, J. F.; Nelson, E. S.; Miller, B. W.; Rolison, D. R.; Long, J. W. *ChemElectroChem* **2016**, *3*, 1369–1375.

[10] The overpotential is the operating potential above the thermodynamic potential for that reaction.

[11] Marshall, A.; Børresen, B.; Hagen, G.; Tsypkin, M.; Tunold, R. *Energy* **2007**, *32*, 431–436.

[12] Walter, M. G.; Warren, E. L.; McKone, J. R.; Boettcher, S. W.; Mi, Q.; Santori, E.A.; Lewis, N.S. *Chem. Rev.* **2010**, *110*, 6446–6473.

[13] McCrory, C. C. L.; Jung, S.; Peters, J. C.; Jaramillo, T.F. *J. Am. Chem. Soc.* **2013**, *135*, 16977–16987.

[14] McCrory, C. C. L.; Jung, Ferrer, I. M.; Chatman, S. M.; Peters, J. C.; Jaramillo, T.F. *J. Am. Chem. Soc.* **2015**, *137*, 4347–4357.

[15] Chen, Y.; Rui, K.; Zhu, J.; Dou, S.X.; Sun, W. *Chem. Eur. J.* **2019**, *25*, 703–713.

[16] Trotochaud, L.; Ranney, J.K.; Williams, K.N.; Boettcher, S.W. *J. Am. Chem. Soc.* **2012**, *134*, 17253–17261.

[17] Louie, M.W.; Bell, A.T. *J. Am. Chem. Soc.* **2013**, *135*, 12329–12337.

[18] Lyu, F.; Wang, Q.; Choi, S.M.; Yin, Y. *Small* **2019**, *15*, 1804201.

low-porosity, nanoparticulate NiFe$_2$Ox was synthesized via a base-catalyzed precipitation method.[19]

We showed that the higher surface area and larger pore volumes associated with the aerogel form of NiFe$_2$Ox provided the lowest overpotential across the series (356 mV at 10 mAcm^{-2}), an ~140 mV improvement over the low surface-area, precipitated analogue (Figure 6) and comparable to the OER activity of previously reported Ni-rich ferrite spinels.[13,16] The OER activity correlated with accessible surface area (increasing from aerogel to xerogel to dense nanoparticles) and not from the hydroxyl content associated with the temperature/atmosphere processing conditions of the catalyst. The pore and solid networks inherent to the aerogel (3D open with > 0.5 cm^3 g^{-1} mesoporous surface area) provide a bicontinuous architecture that allows for facile ingress and egress of reactants and products, thus ensuring high activity.
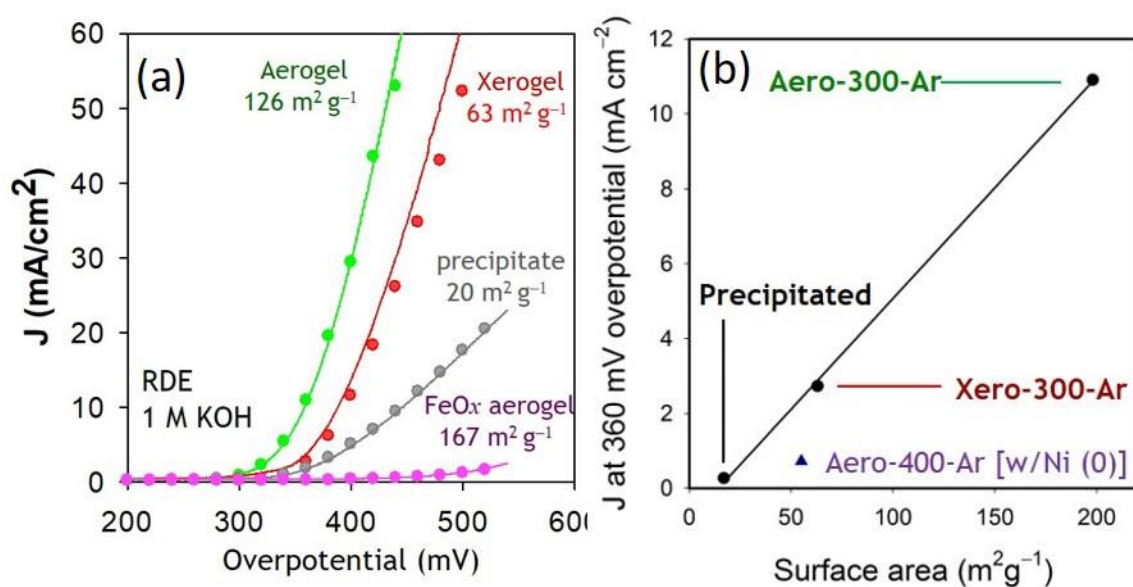
Figure 6. a) Current–overpotential plots at 1600 rpm in O$_2$-purged 1 M KOH in the O$_2$-evolution region of NiFe$_2$Ox/Vulcan carbon and FeOx/Vulcan carbon inks deposited on glassy-carbon rotating disk electrodes. The iR-corrected linear-sweep voltammetric curves (solid lines) were scanned at 10 mV s^{-1} and iR-corrected chronoamperometric points (circles) were collected at steady state after 30 s. b) Specific surface area versus current density at 360 mV overpotential for Aero-300-Ar, Xero-300-Ar, and the precipitated analogue; Aero-400-Ar is also shown but falls outside of the linear relationship because it contains a thermally extruded Ni metal and a lower Ni-to-Fe ratio in the spinel component.

19   Singh, A. A.; Singh, R. N. *Int. J. Hydrogen Energy* **2010**, *35*, 3243–3248.

1B. Bifunctional (OER+ORR) catalysts[20]

Bifunctional OER+ORR catalysts are single nanoscale catalytic materials integrated within the air cathode to minimize the overpotentials of ORR during discharge and OER during recharge. Most catalyst are only active for one of the two reactions, but some of the known OER catalysts, including nickel ferrite spinels, also display ORR activity, creating a compositional phase-space for bifunctionality. In this program, we established Ni-substituted ferrite compositions and morphologies that show bifunctionality. We prepared Ni:Fe spinels ($y = 0.1$ to 0.9 in $Ni_yFe_{1-y}Ox$) using the versatile epoxide-based sol–gel chemistry (see Experiments Section 1A) followed by ambient pressure drying (ambigel)[21,22] or supercritical CO_2 drying (aerogel) to tune both the free volume and the specific surface area of the porous oxide. This series of spinel ferrites allowed us to identify highly active bifunctional compositions and morphologies.[20] All of the $Ni_yFe_{1-y}Ox$ nanoarchitectures in this composition/morphology series were calcined at 350 °C to ensure crystallinity, but the specific oxide crystal structure was composition-dependent. An inverse spinel structure formed for Fe-rich materials ($y \leq 0.33$), rock salt structure for Ni-rich material ($y = 0.9$), and a biphasic structure for intermediate stoichiometry ($0.5 \leq y \leq 0.67$). The morphology of the nickel ferrites as a function of drying technique is summarized in Figure 7.

Material Stoichiometry	Ambigel		Aerogel	
	BET surface area ($m^2\,g^{-1}$)	BJH pore volume ($cm^3\,g^{-1}$)	BET surface area ($m^2\,g^{-1}$)	BJH pore volume ($cm^3\,g^{-1}$)
1 Ni : 9 Fe	73	0.24	107	1.09
1 Ni : 2 Fe	70	0.28	187	1.88
1 Ni : 1 Fe	121	0.31	223	1.4
2 Ni : 1 Fe	153	0.27	231	1.3
9 Ni : 1 Fe	166	0.33	204	0.64
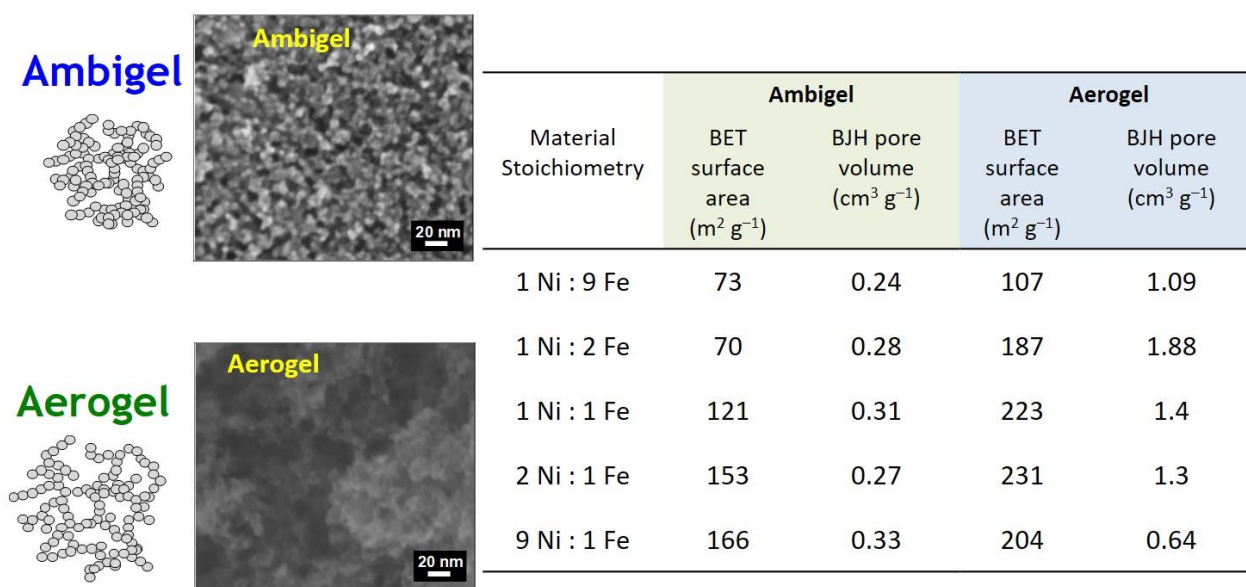
Figure 7. Scanning electron micrographs of representative ambigel and aerogel nickel ferrites and a summary of the surface areas and pore volumes for the compositional range of nickel ferrites.

[20] Ko, J. S.; Chervin, C. N.; Vila, M. N.; DeSario, P. A.; Parker, J. F.; Long, J. W.; Rolison, D. R. *Langmuir* **2017**, *33*, 9390–9397.

[21] Long, J. W.; Swider-Lyons, K. E.; Stroud, R. M.; Rolison, D. R. *Electrochem. Solid-State Lett*. **2000**, *3*, 453−456.

[22] Rolison, D. R.; Dunn, B. *J. Mater. Chem*. **2001**, *11*, 963−980.

Catalytic OER activity for the $Ni_yFe_{1-y}Ox$ series at an overpotential of 390 mV is summarized in Figure 8. The OER current density for the intermediate Ni:Fe stoichiometric range ($0.33 \leq y \leq 0.67$) increased with increasing Ni content and increasing surface area; however, the working curves for ambigel and aerogel OER activity were different. For similar compositions in the intermediate range, we observed comparable OER performance between ambigels and aerogels, but do so with significant differences in their morphology. Ambigels express greater crystallinity and aerogels express larger surface areas demonstrating that OER activity is not simply a function of high surface area or degree of crystallinity for a given composition. These results also show that high OER activity is obtainable with the less expensive ambigel processing technique (i.e., drying the gel without supercritical-fluid extraction) because these sol–gel derived materials retain moderately high surface area and porosity. In this work, we heated the oxides at 350°C in air so that all compositions were crystalline, but ultimately catalyst optimization requires fine-tuning the temperature/atmosphere conditions. For example, the OER ovepotential was improved from 390 to 373 mV at 10 mA cm^{-2} when the $Ni_{0.67}Fe_{0.33}Ox$ aerogel was heat-treated at 300°C/Ar, which we attribute to an increase in crystallite size (2.7 to 4.1 nm) without significant loss of surface area.[20]
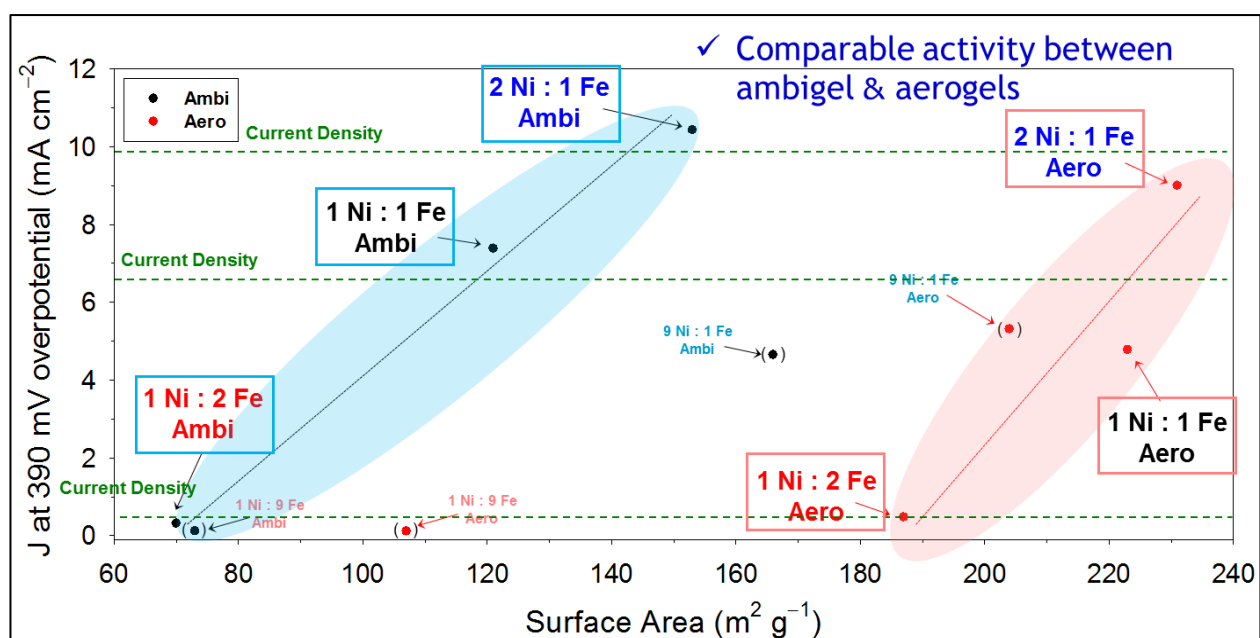
Figure 8. Specific surface area versus oxygen-evolution current density at an overpotential of 390 mV for the 350 °C/air-treated $Ni_yFe_{1-y}Ox$ ambigel and aerogel series prepared as coatings deposited from carbon + catalyst inks.

12

Next, we characterized the ORR activity of the series of ambigel and aerogel $Ni_yFe_{1-y}Ox$ catalysts and determined the stoichiometries and nanoarchitectures that give the highest bifunctional activity at 10 mA cm^{-2}; the metric of high activity is the smallest difference between the OER and ORR overpotentials ($\Delta E_{OER-ORR}$; results summarized in Table 1). Electrocatalytic activity for ORR is greatest for Fe-rich $Ni_yFe_{1-y}Ox$ materials, whereas OER improves with increased Ni composition. Despite Fe-rich compositions providing the highest ORR activity, we determined that with increasing Ni content (greater than 0.5) we retain a two-electron O_2-reduction pathway. The same is not true when considering OER for Fe-rich compositions; in that case, the catalytic activity for OER becomes nonexistent with increasing Fe-content. Thus, starting with the higher performing OER compositions, we can choose a nickel ferrite nanoarchitecture that optimizes OER while maintaining moderate ORR activity to minimize $\Delta E_{OER-ORR}$.

Table 1. Oxygen-Evolution and -Reduction Activity of $Ni_yFe_{1-y}Ox$ Ambigels and Aerogels

Material Stoichiometry	Ambigel			Aerogel		
	ORR η at 1 mA cm^{-2} (mV)	OER η at 10 mA cm^{-2} (mV)	$\Delta E_{OER-ORR}$ (mV)	ORR η at 1 mA cm^{-2} (mV)	OER η at 10 mA cm^{-2} (mV)	$\Delta E_{OER-ORR}$ (mV)
1 Ni : 9 Fe	482	–	–	529	–	–
1 Ni : 2 Fe	497	–	–	512	467	979
1 Ni : 1 Fe	523	397	920	491	404	895
2 Ni : 1 Fe	509	389	898	520	392	912
9 Ni : 1 Fe	506	401	907	501	403	904

OER potentials measured at 10 mA cm^{-2}; ORR potentials measured at –1 mA cm^{-2}.

Program Highlights for Catalyst Design

- Demonstrated high OER activity for Fe-rich nickel ferrite aerogels commensurate with previously reported activity for Ni-rich compositions prepared by conventional techniques
- Obtained highest OER activity (low overpotential at 10 mA cm^{-2}) with Ni-rich nanoarchitectures ($y \geq 0.5$)
- Monitored a monotonic increase in current density with progressively higher surface area for each ambigel and aerogel in the intermediate Ni:Fe stoichiometric range ($0.33 \leq y \leq 0.67$) with aerogels consistently expressing higher surface area

- Correlated the comparable activity at a given Ni:Fe stoichiometry for the ambigel and aerogel expressions to the larger crystallite size present in the ambigels thereby countering lower relative surface area

- Obtained high ORR activity for Fe-rich $Ni_yFe_{1−y}Ox$ materials indicating that selecting an intermediate stoichiometric compromise would provide reasonable OER and ORR electrocatalytic activity (i.e., bifunctionality)

- Established that assessing catalytic activity requires deconvolving the multivariate interplay between Ni:Fe stoichiometry, surface area, crystallographic phase, and crystallite size—no one parameter provides complete predictive power on catalytic performance

2. Practical air-cathode fabrication and electrochemical testing[23]

Zinc–air battery performance is largely determined by the design and functionality of the air-breathing cathode.[6,24,25] Developing an optimized cathode requires three-electrode electroanalytical techniques that benefit from an independent reference electrode and are free from challenges associated with Zn rechargeability. Unfortunately, typical 3-electrode configurations operate in flooded electrolyte conditions that prevent facile flux of O_2 to and from the reaction sites of practical air cathodes, thereby limiting the ability to assess the moderate $10 \, \text{mA cm}^{−2}$ rates of Zn–air batteries. In this program we address this challenge by designing an air-breathing electroanalytical cell that readily assess the air cathode performance (e.g., OER, ORR, pulse-power, and long-term cycling stability) under conditions that mimic operation in a full Z–air battery.[23] The 3D-printed, thermodynamically referenced electroanalytical cell (see Figures 9 and 10) allows for placement of the gas-diffusion working electrode with one side exposed to electrolyte that contains a reference electrode and a counter electrode and the opposing side exposed to a gaseous atmosphere (e.g., flowing or static air or flowing argon).

We demonstrated the utility of our 3D-printed cell for quantifying the steady-state OER and ORR activity of a bifunctional composite air cathode and a
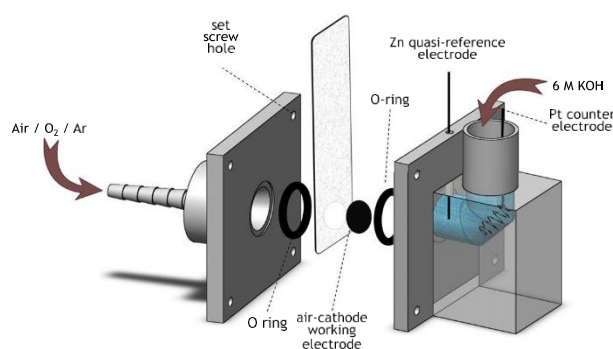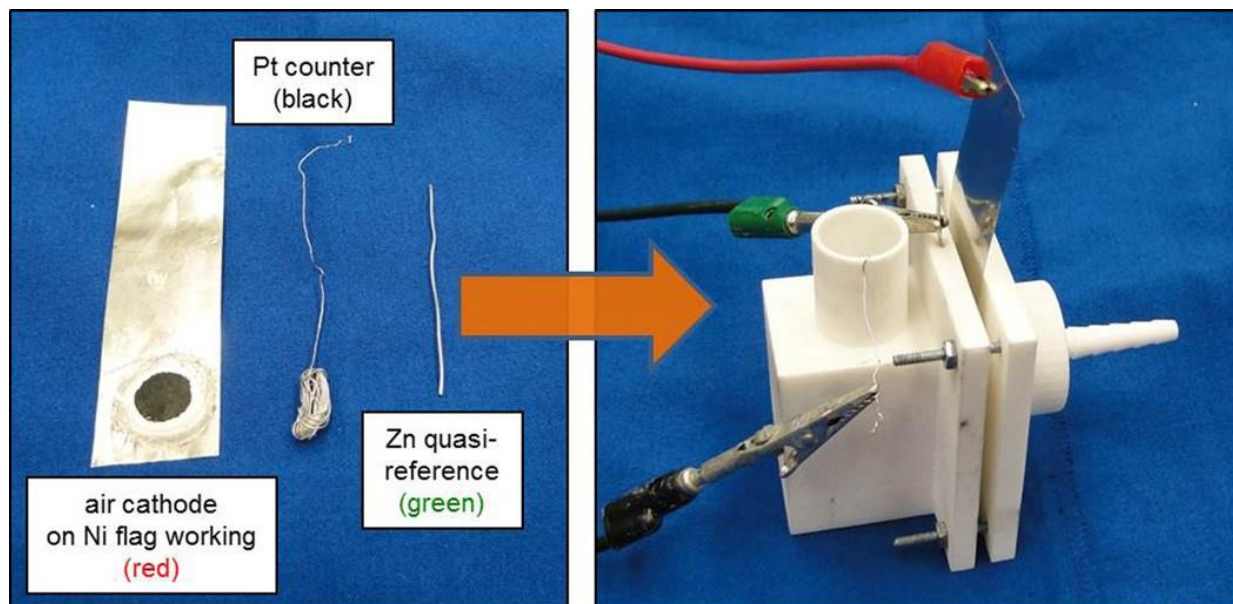

Figure 9. Schematic of the 3D-printable cell used to evaluate gas-diffusion electrodes.

[23] Parker, J. F.; Chervin, C. N.; Nelson, E. S.; Long, J. W.; Rolison D. R. *Nanotechnology* **2016**, *27*, 174002.
[24] Jörissen, L. *J. Power Sources* **2006**, *155,* 23–32.
[25] Neburchilov, V; Wang, H; Martin, J. J.; Qu, W. *J. Power Sources* **2010**, *195*, 1271–1291.

14

Figure 10. (left) Photograph of a composite cathode attached to the Ni flag current collector, Pt counter electrode, and Zn quasi-reference electrode; color labels reference the color of lead attached to the respective electrodes in the photograph on the right. (right) Photograph of the assembled 3D-printed electroanalytical cell.

catalyst-free carbon control (Figure 11) under conditions relevant to Zn–air batteries. The bifunctional composite cathode comprised MnOx for O$_2$ reduction and NiFe$_2$Ox for O$_2$ evolution dispersed within a porous carbon/binder matrix. The air-breathing design of the electroanalytical cell, which supports facile flux of O$_2$ to the porous cathode, allowed us to measure high current densities for O$_2$-reduction and O$_2$-evolution through a potential window that is typical for the Zn–air application (Figure 12). Comparing the bifunctional cathode with the carbon control we observed a 2× enhancement in ORR current density at 1.2 V (typical operating voltage for Zn–air batteries) and a shift in the onset of O$_2$ reduction to more positive potentials (lower overpotential), as is expected for a MnOx-functionalized carbon electrode.[24] The bifunctional cathode also showed higher OER activity than the carbon control, reducing the overpotential by 120 mV at 10 mA cm^{-2} (Figure 12b), which is attributed to the presence of catalytic NiFe$_2$Ox. The results from this work demonstrate that the 3D printed electroanalytical cell is an effective
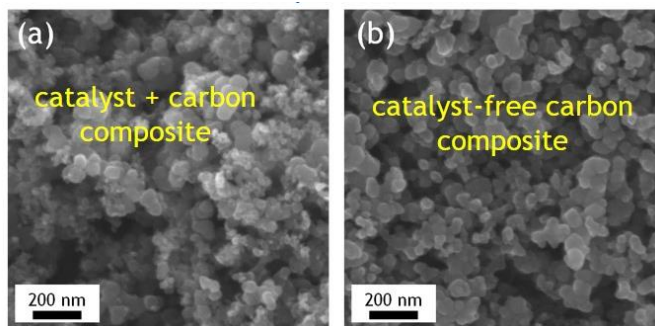
Figure 11. Scanning electron micrographs of (a) MnOx/NiFe$_2$Ox/Vulcan carbon bifunctional cathode and (b) catalyst-free Vulcan carbon composite cathode

screening tool for evaluating bifunctional cathodes at practical current densities for rechargeable Zn–air battery applications.
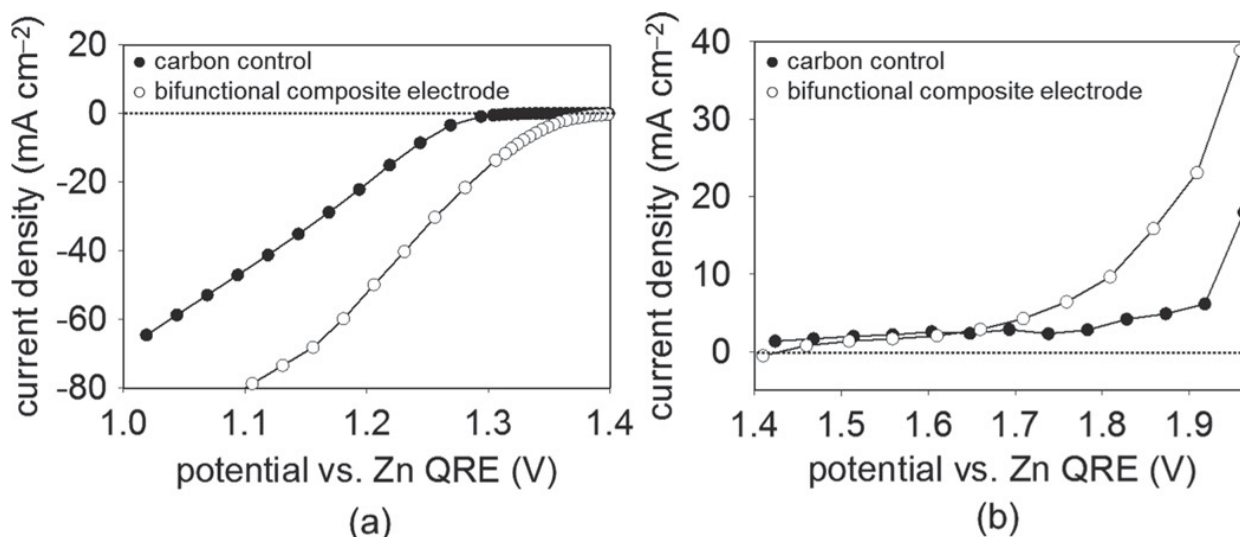
Figure 12. (a) Current–potential responses over the ORR potential window in 6 M KOH electrolyte under static air for (o) MnOx/NiFe$_2$Ox bifunctional powder-composite cathode and (●) Vulcan carbon powder-composite cathode; (b) current–potential responses over the OER potential window in 6 M KOH electrolyte under static air for (o) MnOx/NiFe$_2$Ox bifunctional cathode and (●) Vulcan carbon cathode. All steady-state currents were taken 10 min after each potential step.

3. Practical air cathode electrochemical analysis[26,27]

The exceptional specific energy that might be achieved with rechargeable Zn–air has spurred intense research, much of it focused on the development of the "bifunctional" air cathode needed to electrochemically recharge Zn–air batteries. Yet, unfamiliarity with cell-level considerations may result in reports that mistranslate materials-level or bench-scale test findings when projecting performance in practical zinc batteries. Here we show that results from fundamental studies do not necessarily translate into device-level performance, especially once catalyst morphology and intetgration into practical electrodes are taken into consideration.[26] We also set forth metrics that should be used when testing practical bifunctional cathodes to ensure that the electrodes (and catalysts) are characterized under real-world conditions that are relevant to the high energy density promised by Zn–air batteries.[27]

3A. Catalyst morphology matters in real-world air cathodes

[26] Ko, J. S.; Parker, J. F.; Vila, M. N.; Wolak, M. A.; Sassin, M. B.; Rolison, D. R.; Long, J. W. *J. Electrochem. Soc.* **2018**, *165(11)*, H777–H783.
[27] Parker, J. F.; Ko, J. S.; Rolison, D. R.; Long, J. W. *Joule* **2018**, *2*, 2519–2527.

Manganese oxides (MnOx) are inexpensive, effective electrocatalyst for the oxygen-reduction reaction (ORR) in alkaline media and have seen extensive commercial application in the air cathode of primary Zn–air batteries.[28,29] Because MnOx has a large number of polymorphs and stoichiometries the ORR activity depends on factors that include crystalline structure,[30] particle morphology;[31] oxidation state and defect structure;[32] and surface area of the catalyst and the carbon matrix that supports the catalyst.[6] Nanocrystalline polymorphs of MnO$_2$ with a 2×2 tunnel structure, such as α-MnO$_2$ (cryptomelane), are reported to be the most active catalysts for ORR.[28,29] In this program, we leveraged our previous work with cryptomelane-type MnO$_2$ to demonstrate a critical challenge when transitioning fundamental catalytic research to practical, real-world application; namely, the impact of catalyst morphology and its integration within an electrode matrix. To do so, we synthesized cryptomelane-type MnOx nanoarchtiectres using sol–gel chemistry followed by varying drying methods to produce aerogels, ambigels, and xerogels. The different drying methods varied the pore-solid architecture, but all forms retained the high surface areas (>130 m^2 g^{-1}) that are desirable for electrocatalyst applications.

We demonstrated the importance of catalyst morphology for O$_2$ electrocatalysis in practical electrode configurations and the limitation that fundamental electroanalysis has in accounting for morphological effects.[26] We measured the ORR activity of aerogel and xerogel cryptomelane-type MnOx nanoarchitectures by: (*i*) fundamental electrocatalysis characterization with rotating-disk electrodes (RDEs); (*ii*) applied characterization of practical powder–composite electrodes in our air-breathing three-electrode cell; and (*iii*) device-level characterization of practical air cathodes in Zn–air button cells (Figure 13). Rotating-disk electrode measurements showed that both the aerogel and xerogel MnOx nanoarchitectures have comparable, low onset overpotentials for ORR (~310 mV) and follow the four-electron O$_2$-reduction that is typical for α-MnO$_2$. However, the similarity in performance between the two nanoarchitectures diverges once we go beyond fundamental characterization and integrate the electrocatalyts into the powder-composite form-factors used as air cathodes Zn–air batteries. In this more practical form, the aerogel MnOx morphology showed superior ORR activity in both the air-breathing three-electrode cell and in full

28   Stoerzinger, K. A.; Risch, M.; Han, B.; Shao-Horn, Y. *ACS Catal*. **2015**, *5*, 6021–6031.
29   Meng, Y.; Song, W.; Huang, H.; Ren, Z.; Chen, S.-Y.; Suib, S. L. *J. Am. Ceram.Soc.* **2014**, *136*, 11452–11464.
30   Cao, Y. L.; Yang, H. X.; Ai, X. P.; Xiao, L. F. *J. Electroanal. Chem.* **2003**, *557*, 127–134.
31   Xiao, W.; Wang, D.; Lou, X. W. *J. Phys. Chem. C* **2010**, *114*, 1694–1700.
32   Tang, Q.; Jiang, L.; Liu, J.; Wang, S.; Sun, G. *ACS Catal*. **2014**, *4*, 457–463.

Zn–air button cells (50 to 100 mV lower overpotential at 5–125 mA cm^{-2}). We demonstrated that the improved ORR activity of the aerogel is because it more uniformly disperses within the carbon/binder matrix of the powder composite electrode compared with the xerogel analog, which in turn increases the electroactive surface area for a given weight loading of catalyst. These results demonstrated that fundamental electroanalysis using RDE's, a typical tool for catalyst development, is not a robust way to down-select catalysts because it ignores the impact morphology and fabrication methods have on real-world activity in technologically relevant electrode structures.

18
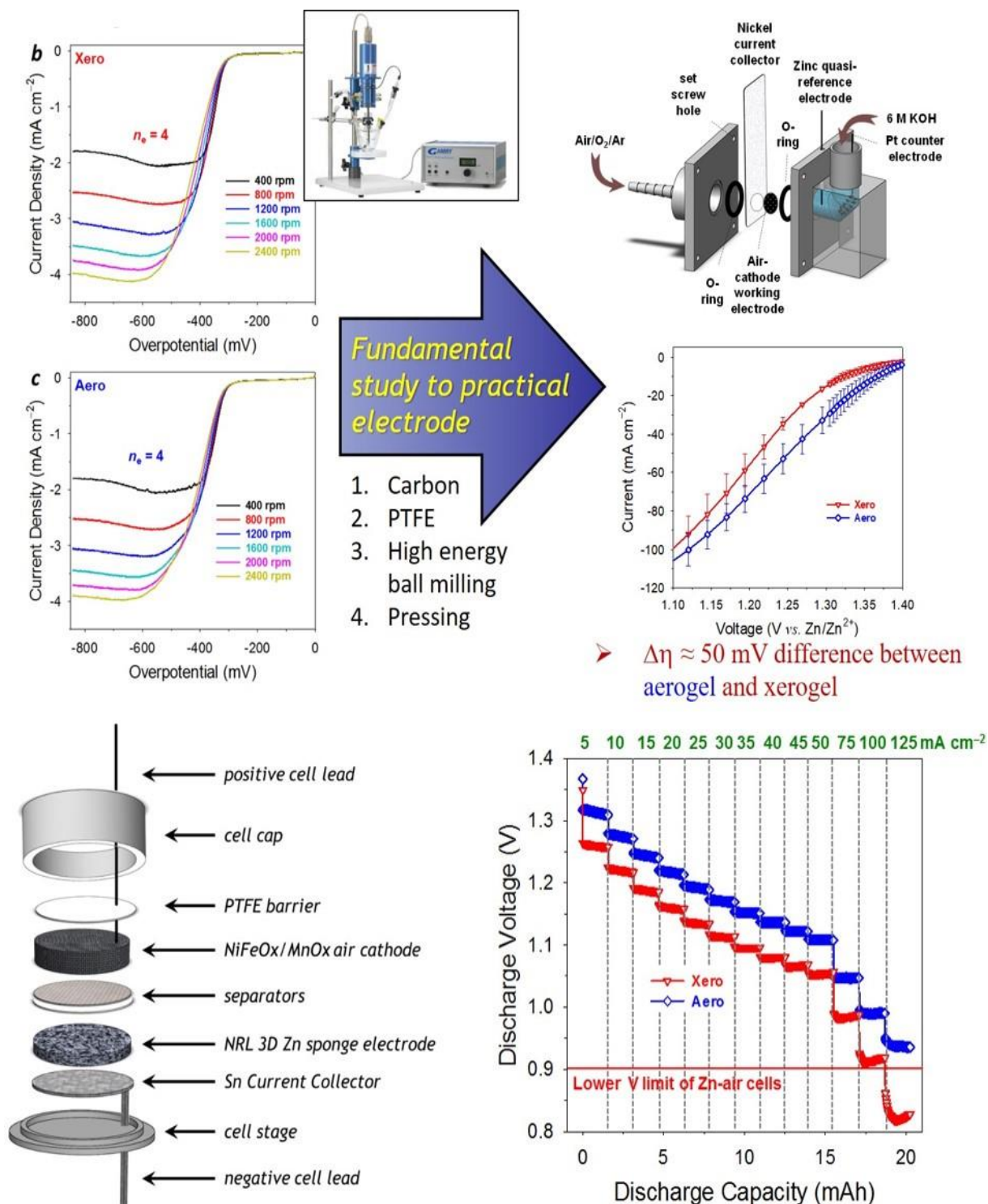
Figure 13. (a) Linear-sweep voltammetric curves at 10 mV s^{-1} in O$_2$-purged 1 M KOH to assess oxygen reduction activity at glassy-carbon rotating disk electrodes for xerogel and aerogel MnOx nanoarchitectures prepared as carbon+catalyst inks; (b) schematic of the air-breathing electroanalytical cell; (c) current–potential response over the oxygen-reduction potential window (1.1–1.4 V vs. Zn/Zn^{2+}) in 6 M KOH under static air for MnOx xerogel and aerogel; (d) schematic of a zinc–air cell using a nylon button-cell configuration and (e) voltage–capacity trends reported at sustained current densities of 5, 10, 25, 50, 100, and 125 mA cm^{-2}.

3B. Translating materials-level performance into device-relevant metrics[27]

Bifunctional cathodes in the literature are usually tested against a Zn foil anode with little or no consideration to the depth of discharge of the Zn anode, yet they include charge–discharge cycling to demonstrated superior cycling performance of the newly designed cathode. The downsides of espousing cycle life in air cathodes is that the cathode itself has infinite capacity (that is, there is an infinite amount of oxygen in the environment for which to reduce). The reported current (or current density) and discharge time define the capacity of the cell per cycle, yet many experiments in those reports fail to push the performance of the air cathodes to a cycling capacity that would balance a zinc anode at technologically relevant specific energy. We have defined a minimum performance metric of an air cathode that, when used, will demonstrate a breakthrough in Zn–air technology.

For an air cathode of area, A in cm^2, cycling at a current density, j in mA cm^{-2}, for individual discharge time, t in hours, the total capacity per discharge can be given simply by:

$$c_{Zn-air} = i \times t = A \times j \times t. \tag{1}$$

The total discharge capacity of a Zn–air battery is defined by the mass of the Zn anode. The anode theoretical capacity in mAh g^{-1} is given as:

$$c_{Zn} = m_{Zn} \times 819.73 = V_{Zn} \times \rho_{Zn} \times 819.73 \tag{2}$$

where V_{Zn} is the volume of the Zn electrode in cm^3 and r_{Zn} is the density of the electrode (for the commonly used foil anode, it is assumed to be the bulk Zn density of 7.14 g cm^{-3}). One can solve for the depth-of-discharge of the Zn electrodes by rationing equations 1 and 2:

$$DOD_{Zn} = \frac{c_{Zn-air}}{c_{T_{Zn}}} = \frac{A_{cathode} \times j \times t}{V_{Zn} \times \rho_{Zn} \times 819.73} = \frac{A_{cathode} \times j \times t}{A_{Zn} \times h_{Zn} \times \rho_{Zn} \times 819.73} \tag{3}$$

To maximize energy density and specific energy of a two-electrode device, one should fix the geometric area of the Zn electrode (A_{Zn}) to match that of the air cathode ($A_{cathode}$) (Figure 15A). In addition, the DOD$_{Zn}$ in a Zn–air battery shall be a minimum of 0.20 in order to meet the technologically relevant threshold of 100 Wh kg^{-1} (Figure 15B). Setting $A_{cathode} = A_{Zn}$, DOD$_{Zn}$ = 0.2, and assigning the thickness of the Zn foil to 0.01 cm (a common thickness for Zn foil anodes), Eq. 3 can be rearranged to define a metric required by a scaled-up, rechargeable Zn–air cell to yield:

$$j \times t_{discharge} \geq 11.7 \text{ mAh cm}^{-2} \text{ (4)}$$

Comparing the requirement defined in Eq. 4 with Zn–air cells in the peer-reviewed literature reveals that the majority fall several orders of magnitude below the threshold for technological relevance. This concept is emphasized in simulated experiments (Figure 15 C,D) where a Zn–air cell is cycled at either 0.4 mAh cm^{-2} or 20 mAh cm^{-2}, the latter of which exceeds the minimum threshold of 11.7 mAh cm^{-2}. The simulated data of Figure 15D projects to a packaged Zn–air cell of 165 Wh kg^{-1} while that in Figure 15C is cycled to such a low capacity that the data does not support a breakthrough in Zn–air technology.
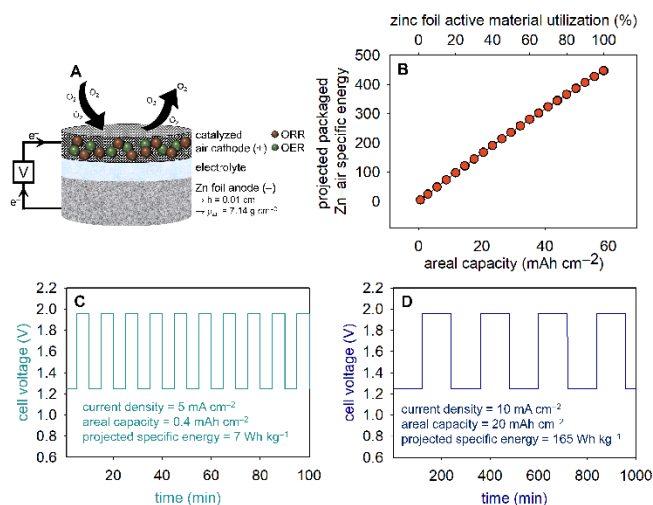
Figure 15. (a) Schematic of a zinc-air cell. (b) Plot of projected Zn–air specific energy as a function of the areal capacity (bottom axis) and the DOD$_{Zn}$ for 0.01-cm-thick Zn foil (top axis). (c) Simulated rechargeable Zn–air full cell operated at 0.4 mAh cm^{-2} and 5 mA cm^{-2}, which projects to a specific energy of 7 Wh kg^{-1}. (d) A similar Zn–air cell operated at and 20 mAh cm^{-2} and 10 mA cm^{-1}, exceeding the minimum threshold of 11.7 mAh cm^{-2} and projecting to a packaged cell of 165 Wh kg^{-1}. The low areal capacity in (c) does not support a breakthrough in Zn–air rechargeability.

Program highlights for fundamental to practical cathodes

- Sol–gel-derived MnOx nanoarchitectures exhibit a full four-electron reduction of molecular oxygen with comparable intrinsic ORR activity and low onset overpotential (~310 mV)

- Aerogel-based composite electrode exhibits an overpotential lowered by ~60 mV compared to the xerogel-based analog

- Aerogel-based composite electrode yields up to 100 mV improvement in discharge voltage at moderate-to-challenging current densities (5–125 mA cm^{-2}) without breaching the cut-off voltage of 0.9 V, which the xerogel-based composite electrode cannot manage

- Attributed the enhanced activity of the cryptomelane MnOx aerogel-based composite to more uniform dispersion of the less dense aerogel powder within the carbon/binder matrix, as verified by microscopic imaging of focused-ion-beam cross-sectioning of the aerogel-based and xerogel-based composites and energy-dispersive spectroscopic mapping.

- Optimized choice of carbon in composite air cathodes that contain at least one nanoarchitectured catalyst and down-selected acetylene black as the carbon of interest for follow-on studies

- Described appropriate means by which to translate materials- and component-level performance into device-level metrics so that future reports on rechargeable Zn-based batteries can stand as technology enablers.

4. Bilayer air cathodes – Integrating pulse-power in composite air cathodes

The final step of cathode development in this program was to fabricate a bilayer cathode that combines the pulse-power capabilities of MnOx-functionalized carbon nanofoam papers with the ORR and OER functionality of the composite cathodes demonstrated in Experiments Section 3. The bilayer cathode is a laminated structure comprising a functionalized carbon nanofoam "glued" to a pre-formed carbon composite cathode prepared using our standard fabrication techniques. Lamination is achieved by simply pressing the nanofoam to the carbon composite, or for a more intimate connection, a mixture of hydrophilic binder, water, and acetylene black carbon is prepared as a conductive glue to bind the two layers. Using the air-breathing electroanalytical cell described in Experiments Section 2, we demonstrated that the bilayer architecture retains the O$_2$-electrocatalytic behavior of the carbon composite while also delivering O$_2$-independent pulse power that is otherwise unachievable with the carbon composite cathode (Figure 14). These results demonstrate that we can pre-form a catalyst layer separate from the pulse-power delivering nanofoam; the direct benefits of this approach are: (*i*) flexible catalyst choice; (*ii*) inexpensive scale-up; (*iii*) leverage established fabrication protocols for gas-diffusion electrodes; (*iv*) tune
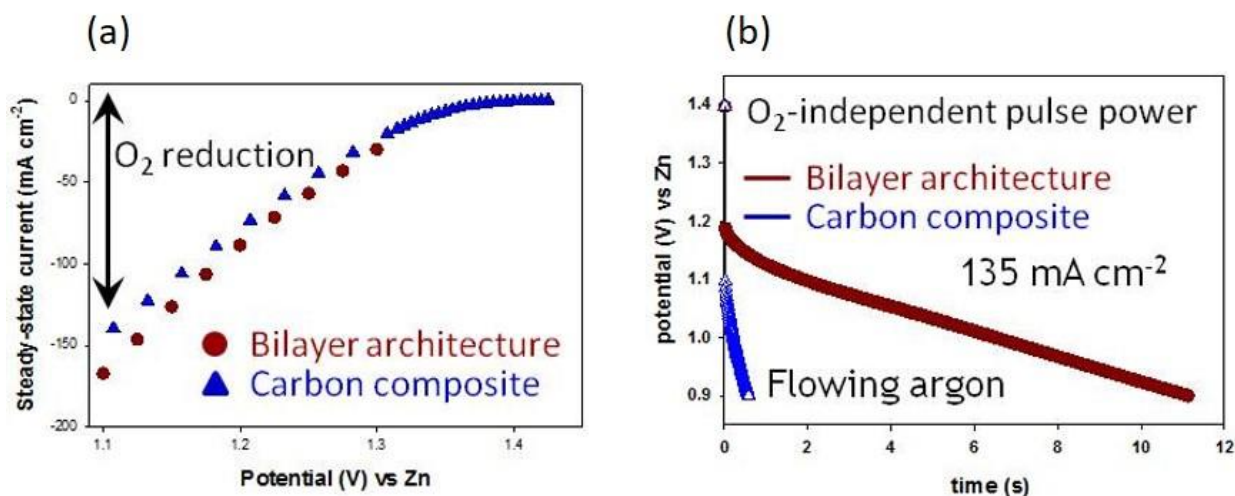
Figure 14. Three-electrode air-breathing cell experiments in 6 M KOH demonstrating that a bilayer cathode comprising a MnOx-modified carbon nanofoam layer laminated to a catalyzed carbon composite layer exhibits the pulse-power functionality of the nanofoam. (a) steady-state ORR activity of a carbon-composite cathode and a bilayer nanofoam-composite cathode; (b) O$_2$-free galvanostatic pulse at 135 mA cm^{-2} under flowing Ar of a carbon composite cathode and a bilayer nanofoam-composite cathode.

pulse-power capability by optimizing MnOx loading and nanofoam thickness, porosity, and hydrophilicity.

5. Advances in 3D zinc "sponge" anodes for rechargeable Zn–air batteries. [33]

While the primary research focus of this program was to develop advanced bi- and tri-functional air cathodes, realizing high-performance rechargeable Zn–air batteries also requires Zn anodes that exhibit dendrite-free cycling, high gravimetric and volumetric capacity, and high-power capability. As noted above, early demonstrations with "Gen 1" NRL Zn sponges,[3,4] including in primary Zn–air cells, motivated efforts to apply more dense Zn sponges in rechargeable Zn–air configurations. During the course of this 6.2 program, we had the opportunity to leverage other ONR funding to further optimize the structure and performance of Zn sponges.[33] A shortcoming of the Gen-1 sponge was its relatively low density ($\sim$20% solid), which limited volumetric capacity and resulted in sub-optimal mechanical strength. To overcome these challenges, we reformulated the precursor Zn powder feedstock with a mixture of particle sizes, ultimately resulting in a "Gen 2" sponge architecture that increases the total solid volume fraction up to 28–30% zinc.[33] Enhanced mechanical integrity of the dense sponge allows for routine handling of Gen-2 sponges down to 500-μm thick, while the higher density increased volumetric capacity by 50% vs. the Gen-1 sponge. In the 2019 *ACS Applied Energy Materials* paper where we describe the fabrication and testing of Gen-2 Zn sponges, we also reported characterization by X-ray computed tomography, which confirmed the 3D continuity of the Zn solid network (see Figure 16).[33] In the latter stages of the present 6.2 Zn–air program, the Gen-2 Zn sponge served as the workhorse anode in the prototype rechargeable Zn–air cells that are described below.

---

[33] Ko, J. S.; Geltmacher, A. B.; Hopkins, B. J.; Rolison, D. R.; Long, J. W.; Parker, J. F. *ACS Appl. Energy Mater.* **2019**, *2*, 212–216.
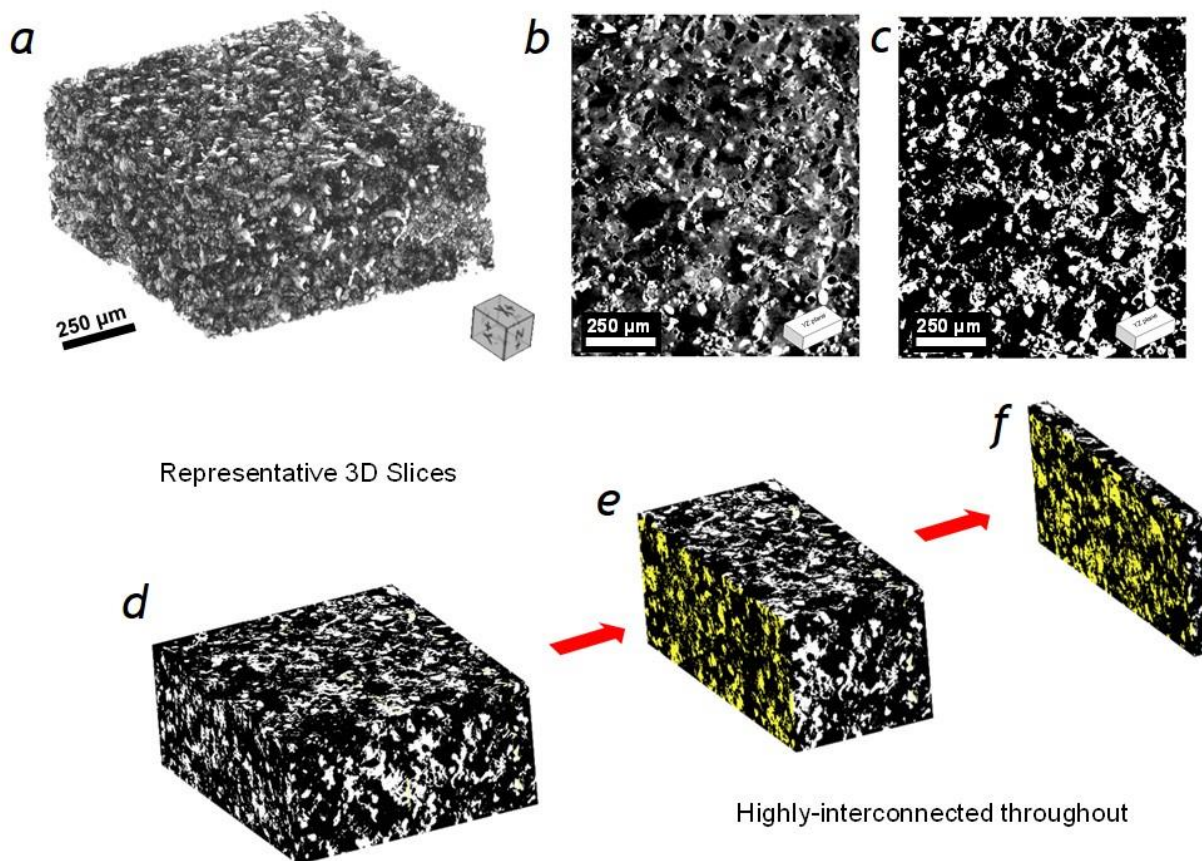
Figure 16. The 3D volume–rendered X-ray tomogram of **(a)** Zn_{20} and **(d)** Zn_{30} sponges and individual slice (YZ–plane) perpendicular to the electrode thickness of **(b)** Zn_{20} and **(e)** Zn_{30}. Binarized image of **(c)** Zn_{20} from the individual slice (YZ–plane) thresholded to yield a volume fraction of $\sim 25\,\%$ and of **(f)** Zn_{30} to yield a volume fraction of $\sim 30\,\%$. The 3D volume of the macroscopic sponge was reconstructed with defined dimensions ($\sim 750\,\mu m \times \sim 500\,\mu m \times \sim 750\,\mu m$) and trimmed on all six sides to reduce artifacts present in the tomography scans arising from beam hardening and edge effects. Scans were performed with a resolution corresponding to $1.2\,\mu m$ voxel size.

6A. Prototype Rechargeable Zn–air cells[34,35]

The final phase of this program was to pair our air cathode designs with NRL's 3D Zn sponge anode in prototype recheargheable Zn–air cells. Using a Zn–air cap cell (Figure 17; laboratory version of a coin cell), we demonstrated full recharge over many discharge–charge cycles. The cells comprised a Zn sponge anode and a $Ni_yFe_{1-y}Ox/MnOx$-catalyzed carbon composite cathode as described in Experiments Section 2. The rechargeable coin-type cells were assembled and cycled to 20 to 40% depth of discharge of the Zn anode (DOD_{Zn}), which corresponds to

---

[34] Patent Application: Parker, J. F.; Long, J. W.; Rolison, D. R.; Chervin, C. N. Rechargeable Zinc/Air Batteries. October 25, 2018 [Navy Case #106,342].

[35] Chervin, Long, Rolison, Parker, Hopkins, Ko, Hoffmaster – In preparation

~150 W h kg^{-1} when translated to a practical device.[27] The galvanostatic discharge–charge cycling at 10 mA cm^{-2} for a typical Zn–air cell is shown in Figure 18a. In this example, the bifunctional gas-diffusion cathode was fabricated with a 10/10/65/15 weight ratio of MnOx/NiFe$_2$Ox/conductive carbon/PTFE and 12 M KOH was used as the electrolyte. The initial discharge was set to 37.7 mA h (40% DOD$_{Zn}$) and all subsequent charge–discharge steps were limited to a nominal capacity of 28.3 mA h (30% DOD$_{Zn}$). The first cycle was discharged 9.4 mA h more than the subsequent cycles in order to impart a buffering amount of potassium zincate into the electrolyte solution and to prevent overcharge during the constant-current 10 mA cm^{-2} charge steps. For this example, the cell achieved 20 charge–discharge cycles before falling below 80% of the nominal capacity, or a total of 535.4 mA h, or nearly 6× the total theoretical capacity (i.e., full oxidative utilization) of the Zn electrode, demonstrating the full rechargeability of the cell because the multiple cycles we achieved at this DOD$_{Zn}$ would exhaust the total amount of Zn present multiple times unless recharging of the depleted Zn occurs.
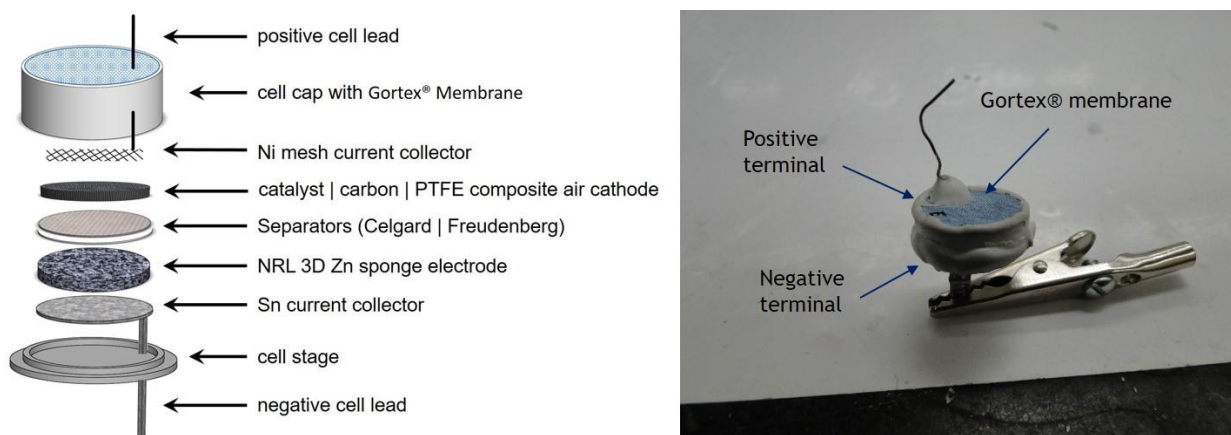
Figure 17. (a) Schematic of a "cap" cell used for testing full rechargeability of Zn paired against an air cathode in a Zn–air battery configuration; (b) photograph of an assembled Zn–air cap cell.

25

To further demonstrate that an equivalent of the Zn sponge anode greater than 100% of the total amount of Zn in the sponge is discharged and then recharged for subsequent use, we poised a cell to cycle at lower rate and lower depth of discharge but over more cycles (Figure 18b). We used a cell configuration with a 20/20/45/15 weight ratio of MnO_x/$Ni_{0.75}Fe_{0.25}O_x$/conductive carbon/PTFE in 9 M KOH run at 5 mA cm^{-2} set to consume an average of 15% DOD$_{Zn}$. The cell achieved 30 charge–discharge cycles before falling below 80% of the nominal capacity, or a total of 637 mA h, or nearly 8× total theoretical capacity of the Zn electrode, indicating successful recharging of both electrodes.
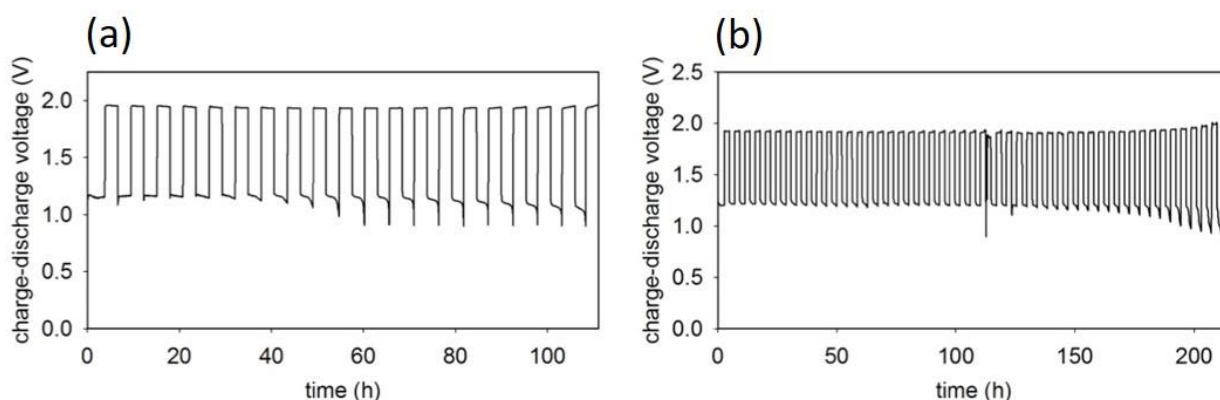
Figure 18. Galvanostatic discharge–charge of Zn–air cells under varied conditions: (a) 10 mA cm^{-2} in 12 M KOH at 40% DOD$_{Zn}$ for 1st discharge and 30% DOD$_{Zn}$ for subsequent discharge steps; (b) 5 mA cm^{-2} in 9 M KOH at 20% DOD$_{Zn}$ for 1st discharge and 15% DOD$_{Zn}$ for subsequent discharge steps.

6B. Optimizing air cathodes in rechargeable Zn–air cells

The discharge–charge voltage hysteresis (ΔV), which is the difference between the average charging and discharging voltages at a given current density, is a measure of catalytic effciency of the air cathode. Although the cathode efficiency is dependent on a number of factors, the choice of catalyst is paramount. In this program we fabricated Zn–air cells with different cathode catalyst configurations and determined the ΔV over 20 discharge–charge cycles at 10 mA cm^{-2}. Selecting two aerogel–derived metal-oxide catalysts in which the activity for one is optimized for oxygen reduction and the other for oxygen evolution and then combining them into a composite air cathode results in a ΔV less than 700 mV in Zn–air cells (Figure 19a). Such hysteresis values are not only among the lowest reported in the literature, but also a rare example of electrocatalyst performance validated in a practical Zn–air cell configuration at technologically relevant current density and cell capacity. We have also established that NRL's nickel-ferrite aerogel catalysts express

bifunctional catalytic function, i.e., they can effectively catalyze the battery charge and discharge reactions (Figure 19b). When incorporated into powder-composite air cathodes and tested in prototype rechargeable Zn–air cells, these bifunctional nickel-ferrite catalytic architectures perform nearly as well as cathodes made with separate charge and discharge catalysts (720 vs 690 mV voltage hysteresis).
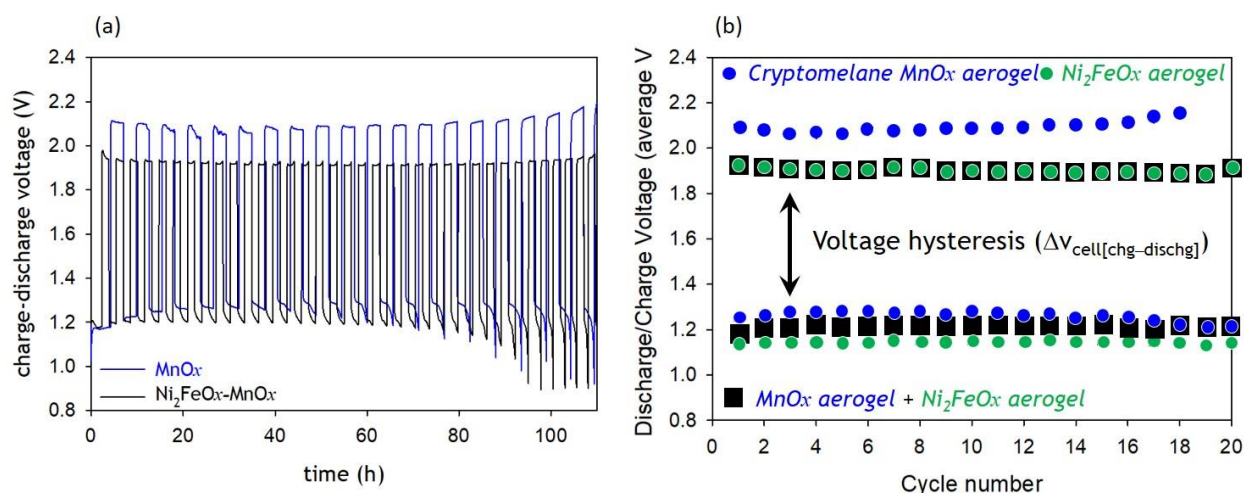
Figure 19. (a) Galvanostatic discharge–charge cycling at 10 mA cm^{-2} and 20% DOD$_{Zn}$ of Zn–air cells utilizing (—) Ni$_2$FeOx-MnOx or (—) MnOx composite cathodes paired with Gen-2 Zn sponge anodes; (b) average discharge and charge voltages for Zn–air cells with different cathode compositions: Ni$_2$FeOx; Ni$_2$FeOx-MnOx; or MnO$\underline{x}$.

6C. Best Performing Zn–air Cells[35]

Using a down-selected composite cathode (Ni$_2$FeOx/MnOx catalysts) and our Generation-2 Zn sponge anode described in Experiments Section 5 we have demonstrated a Zn–air cell that cycled for almost 50 cycles at a specific energy of 150 W h kg^{-1} (comparable to Li-ion) at 10 mA cm^{-2} (Figure 20). The causes of capacity fade and eventual cell failar are not definitively known, but there is evidence of a thick film on the surface of the air cathode at the
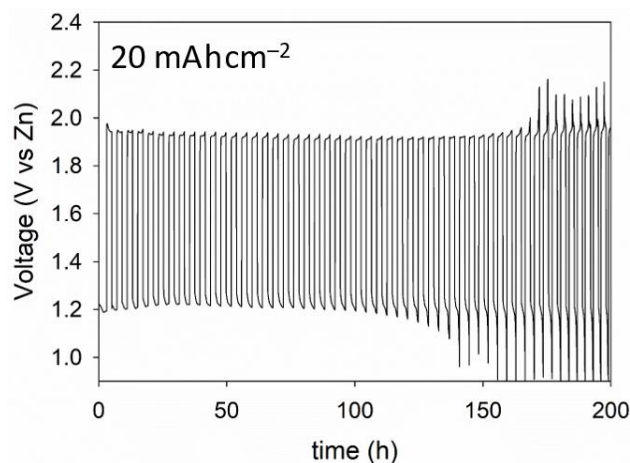
Figure 20. Galvanostatic discharge–charge cycling at 10 mA cm^{-2} and 20% DOD$_{Zn}$ of a Zn–air cell comprising a Gen-2 Zn sponge anode and a composite cathode with Ni$_2$FeOx and MnOx catalysts.

interface with the separator. We propose that $O_2(g)$ build-up at the cathode/separator interface during charging (O_2-evolution at the cathode) promotes precipitation of various compounds, including ZnO   (Zn–air battey electrolytes become saturated with zincate as a normal course of charge–discharge), potassium hydroxide from the electrolyte, and potassium carbonate as a side reaction of atmospheric CO_2 and the alkaline electrolyte. The white film is visible by eye following post-cycle cell disassembly.   Scanning electron microscopy coupled with energy-dispersive spectroscopy indicates a thick region rich in Zn and a second

Figure 22. (Top and bottom right) SEM/EDS characterization of a showing separation of Zn-based precipitates and K-based precipitates; (bottom left) X-ray diffraction of the post-cycled composite cathode with Ni_2FeO_x and MnO_x catalysts showing distinct peaks that index to ZnO. The smaller peaks are an unknown phase.

thinner region rich in potassium (see Figure 21). The Zn region is confirmed by X-ray diffraction (XRD) to be ZnO (see Figure 22); whereas the potassium-rich region, not observed as a distinct crystalline phase by XRD, is shown to be a mixture of potassium oxy(hydroxide) and potassium carbonate by X-ray photoelectron spectroscopy (data not shown).

Figure 21. SEM/EDS characterization of a post-cycled composite cathode with Ni_2FeO_x and MnO_x catalysts showing separation of Zn-based precipitates and K-based precipitates.

FUTURE WORK

The next steps to achieve a rechargeable Zn–air battery with pulse-power capability is to combine the individual accomplishments of the trifunctional air cathode and then integrate it

within a full Zn–air cell. Preliminary work during this program illuminated an initial challenge to this next step. We found that the internal cell resistance of our coin cells, although not large enough to inhibit normal discharge and charge currents (~10–25 mA cm^{-2}), is significantly high to inhibit the high-current pseudocapacitve pulses (>100 mA cm^{-2}) from the MnOx-functionalized nanofoam layer. To solve the resistance problem, the cell must be designed with additional electrical contact to the pulse-power-delivering layer.

In addition to incorporating pulse power, further optimization of cell components is required to extend the Zn–air cycle performance. High priority should be placed on: (*i*) electrolyte management; (*ii*) minimizing bubble formation at the air cathode|separator interface during OER; (*iii*) optimizing compression of cell to minimize series resistance; (*iv*) introduction of gel-based electrolytes to minimize flooding in the air cathode; and (*v*) developing methods to prevent drying out of the separators or cathode at the cathode|separator interface.

Program Productivity (as of November 2019)

Publications

Title: (INVITED) CAD/CAM-designed, 3D-printed electroanalytical cell for the evaluation of nanostructured gas-diffusion electrodes.
Authors: C. N. Chervin, J. F. Parker, E. S. Nelson, D. R. Rolison, and J. W. Long
Type of Publication: (Peer-reviewed journal) Volume **27**, Article Number 174002
Where it Appeared: *Nanotechnology*
Publication Date: February 2016

Title: Minimizing Shape Change at Zn Sponge Anodes in Rechargeable Ni–Zn cells: Impact of Electrolyte Formulation
Authors: J. F. Parker, I. R. Pala, C. N. Chervin, J. W. Long, and D. R. Rolison
Type of Publication: (Peer-reviewed journal) Volume **163**, Pages A353– A355
Where it Appeared: *Journal of the Electrochemical Society*
Publication Date: March 2016 (doi: 10.1149/2.1001602jes).

Title: Next-Generation Rechargeable Zinc Batteries Based on Advanced 3D Electrode Designs
Authors: J. W. Long, J. F. Parker, C. N. Chervin, and D. R. Rolison
Type of Publication: (Peer-reviewed conference proceedings) Volume **35**, Pages 360–363
Where it Appeared: *Proceedings of the 47th Power Sources Conference*
Publication Date: August 2016

Title: Aerogel Architectures Boost Oxygen-Evolution Performance of $NiFe_2Ox$ Spinels to Activities Commensurate with Nickel-Rich Oxides
Authors: C. N. Chervin, P. A. DeSario, J. F. Parker, E. S. Nelson, B. W. Miller, D. R. Rolison, and J. W. Long
Type of Publication: (Peer-reviewed journal: *Journal-designated Very Important Paper and cover art*) Volume **3**, Pages 1369–1375
Where it Appeared: *ChemElectroChem*
Publication Date: September 2016

Title: Rechargeable Nickel–3D Zinc Batteries: An Energy-Dense, Safer Alternative to Lithium-Ion
Authors: J. F. Parker, C. N. Chervin, I. R. Pala, M. Machler, M. F. Burz, J. W. Long, and D. R. Rolison
Type of Publication: (Peer-reviewed journal) Volume **356**, Pages 415–418
Where it Appeared: *Science*
Publication Date: April 2017

Title: (**INVITED**) Electroanalytical Assessment of the Effect of Ni:Fe Stoichiometry and Architectural Expression on the Bifunctional Activity of Nanoscale $Ni_yFe_{1–y}Ox$
Authors: J. S. Ko, C. N. Chervin, M. N. Vila, P. A. DeSario, J. F. Parker, J. W. Long, and D. R. Rolison
Type of Publication: (Peer-reviewed journal; selected for cover art) Volume **33**, Pages 9390–9397
Where it Appeared: *Langmuir*
Publication Date: September 2017 (doi: 10.1021/acs.langmuir.7b01046)

Title: (EDITOR'S CHOICE PAPER) Electrocatalyzed Oxygen Reduction at Manganese Oxide Nanoarchitectures: From Electroanalytical Characterization to Device-Relevant Performance in Composite Electrodes
Authors: J. S. Ko, J. F. Parker, M. N. Vila, M. A. Wolak, D. R. Rolison, and J. W. Long
Type of Publication: (Peer-reviewed journal, Electrochemical Society) Volume **165**, Pages H777–H783, DOI: 10.1149/2.1351811jes
Where it Appeared: *Journal of the Electrochemical Society* [18-1231-2644]
Publication Date: November 2018

Title: (INVITED) Translating Materials-Level Performance into Device-Relevant Metrics for Zinc-Based Batteries
Authors: J. F. Parker, J. S. Ko, D. R. Rolison, and J. W. Long
Type of Publication: (Peer-reviewed journal, Cell Press) Volume **2**, Pages 2519–2527, DOI: 10.1016/joule.2018.11.007
Where it Appeared: *Joule* [18-1231-4769]
Publication Date: December 2018

Title: Robust 3D Zn Sponges Enable High-Power, Energy-Dense Alkaline Batteries
Authors: J. S. Ko, A. B. Geltmacher, B. J. Hopkins, D. R. Rolison, J. W. Long and J. F. Parker
Type of Publication: (Peer-reviewed journal, American Chemical Society) Volume **2**, Pages 212–216, DOI: 10.1021/acsaem.8b01946
Where it Appeared: *ACS Applied Energy Materials* [18-1231-3652]
Publication Date: March 2019

Patents

Title: Rechargeable Zinc/Air Batteries
Inventors: J. F. Parker, J. W. Long, D. R. Rolison, and C. N. Chervin
Type of Publication: US Patent Application (S/N 16/171,251), Navy Case # 106,342
Publication Date: 25 October 2018

Title: (Dense) Zinc Electrodes for Batteries
Inventors: D. R. Rolison, J. F. Parker, and J. W. Long
Type of Publication: PCT Patent Application, Navy Case nr. 102,317-US5 and #106,415
Publication Date: 30 October 2018

Title: Free-Standing Carbon Nanofoams with Graded/Gradient Pore Structure
Inventors: M. B. Sassin, J. W. Long, and D. R. Rolison
Type of Publication: Provisional Patent Application, Navy Case #109,498 [18-1231-4286]
Date: November 2018

Title: Zinc Electrodes for Batteries: Zinc Sponges as a Negative Electrode in Rechargeable Nickel–Zinc Batteries

Authors: J. F. Parker, J. W. Long, and D. R. Rolison
Type of Publication: U.S. Patent Application—Continuation in Part
Where it Appeared: USPTO **US2017-331104-A1**
Submission Date: 3 August 2017

Title: Zinc Electrodes for Batteries: Zinc Sponges as a Negative Electrode in High-Power Silver–Zinc Batteries
Authors: J. F. Parker, J. W. Long, and D. R. Rolison
Type of Publication: U.S. Patent Application—Continuation in Part
Where it Appeared: USPTO **US2017-338479-A1**
Submission Date: 3 August 2017

Title: Rechargeable Zinc/Air Batteries Enabled by 3D Zinc Sponge Anode and an Air Cathode Containing Nanoarchitectured Oxygen Reduction and Evolution Electrocatalyst
Authors: J. F. Parker, J. W. Long, D. R. Rolison, and C. N. Chervin
Type of Publication: U.S. Provisional Patent Application
Where it Appeared: USPTO **Navy Case #106,342**
Submission Date: 26 October 2017

Title: Dense Zinc Sponge Electrodes for Batteries with High Volumetric Energy
Authors: D. R. Rolison, J. F. Parker, J. S. Ko, and J. W. Long
Type of Publication: U.S. Patent Application—Continuation in Part
Where it Appeared: USPTO **US2017-0338479**
Submission Date: 30 October 2017

Title: Zinc Electrodes for Batteries
Authors: D. R. Rolison, J. F. Parker, and J. W. Long
Type of Publication: U.S. Patent #**9,802,254**
Where it Appeared: USPTO
Publication Date: 31 October 2017

Recognition

1. J. F. Parker, J. W. Long, D. R. Rolison: Dr. Delores M. Etter Top Scientists & Engineers Team Award, presented 22 June 2016
2. C. N. Chervin and E.S. Nelson, 2016 Division of Inorganic Chemistry Award for Undergraduate Research
3. J. F. Parker, *PECASE* (2017)
4. D. R. Rolison: Appointed Editorial Advisory Board for *Advanced Energy Materials*, 2014 to present
5. D. R. Rolison: Appointed Editorial Advisory Board for *Chemical Reviews*, 2016 to present

6. D. R. Rolison: Appointed Editorial Advisory Board for *ACS Applied Energy Materials*, 2016 to present

7. D. R Rolison, Member, Selection Committee for MRS Fellows (2017)

8. D. R. Rolison, J. F. Parker, and J. W. Long: NRL Edison Patent Award for "Zinc Electrodes for Batteries" (U.S. Patent #10,008,711); presented in April 2019

9. D. R. Rolison: Chair: Selection Committee for Fellows of the Materials Research Society, (20187–2019)

10. D. R. Rolison: Editorial Advisory Board for *ACS Applied Energy Materials* (2018–present)

11. D. R. Rolison: Elected, Council Delegate, American Association for the Advancement of Science (2019–2021)

12. D. R. Rolison: External Advisory Board for the UCLA–led DOE–funded Energy Frontiers Research Center on Synthetic Control Across Length-scales for Advancing Rechargeables (SCALAR), Los Angeles, CA (2018–present)

Additional Information

—*Presentations*

1. (INVITED) "3D Zn Sponge Anodes Enable Rechargeable Zinc-Based Alkaline Batteries." D. R. Rolison, J. F. Parker, C. N. Chervin, J. W. Long [NRL] and M. B. Burz [EnZinc], Telebriefing to Mr. Chad Allison, Mahindra/GenZe, 6 October 2015.

2. (INVITED) "The Road Beyond Lithium Batteries Is Paved—In Three Dimensions—With Rechargeable, Dendrite-Free Zinc." D. R. Rolison, J. F. Parker, C. N. Chervin, I. R. Pala, M. D. Wattendorf, and J. W. Long in the session on Batteries and Supercapacitors, AVS 62nd International Symposium & Exhibition, 18–23 October 2015, San Jose, CA.

3. "Architectural Design In 3D Physically Thwarts Dendrite Formation—With Zinc Now Rechargeable, Who Needs Lithium Batteries?" D. R. Rolison, J. F. Parker, I. R. Pala, C. N. Chervin, E. S. Nelson, M. D. Wattendorf, and J. W. Long in the symposium on Materials and Architectures for Safe and Low-Cost Electrochemical Energy-Storage Technologies, Fall Meeting of the Materials Research Society, Boston, MA, 29 November–4 December 2015.

4. (INVITED) "High-Performance Next-Generation Electrochemical Power Sources," J. W. Long, C.N. Chervin, M.B. Sassin, J.F. Parker, and D.R. Rolison, Briefing to Dr. Andrew Higier, Associate Director, Office of Naval Research–Global, U.S. Naval Research Laboratory, Washington, DC, 4 January 2016.

5. (INVITED) "High-Performance Next-Generation Electrochemical Power Sources." <u>D. R. Rolison</u>, J. W. Long, C. N. Chervin, M. B. Sassin, and J. F. Parker, Briefing to Representatives of the Naval Acquisitions Development Program, U.S. Naval Research Laboratory, Washington, DC, 14 January 2016.

6. (INVITED) "High-Performance Next-Generation Electrochemical Power Sources." <u>C. N. Chervin</u>, <u>J. F. Parker</u>, <u>J. W. Long</u>, <u>M. B. Sassin</u>, and <u>D. R. Rolison</u>, Briefing to Dr. Mark Borden, Defense Intelligence Agency, U.S. Naval Research Laboratory, Washington, DC, 21 January 2016.

7. (INVITED) "High-Performance Next-Generation Electrochemical Power Sources." <u>J. W. Long</u>, J. F. Parker, C. N. Chervin, M. B. Sassin, and D. R. Rolison, Briefing to Mr. Billy Short, Office of Naval Research, U.S. Naval Research Laboratory, Washington, DC, 29 January 2016.

8. (INVITED) "Architectural Design In 3D Physically Thwarts Dendrite Formation—With Zinc Now Rechargeable, Who Needs Lithium Batteries?" <u>D. R. Rolison</u>, J. F. Parker, C. N. Chervin, and J. W. Long, Briefing to Dr. Allison Fisher, FlexEl, Inc., U.S. Naval Research Laboratory, Washington, DC, 3 February 2016.

9. (INVITED) "Architectural Design In 3D Physically Thwarts Dendrite Formation—With Zinc Now Rechargeable, Who Needs Lithium Batteries?" <u>D. R. Rolison</u>, J. F. Parker, C. N. Chervin, and J. W. Long, Telebriefing to Lt. Commander Jason Fahy, CNO Strategic Studies Group, 8 February 2016.

10. (INVITED) "Architectural Design In 3D Physically Thwarts Dendrite Formation—With Zinc Now Rechargeable, Who Needs Lithium Batteries?" <u>D. R. Rolison</u>, J. F. Parker, C. N. Chervin, and J. W. Long, Briefing to Dr. John Kotek, Acting Assistant Secretary, Office of Nuclear Energy, U. S. Naval Research Laboratory, Washington, DC, 26 February 2016.

11. "Rechargeable Zinc–Air Batteries with Pulse-Power Capability." <u>C. N. Chervin</u>, J. W. Long, J. F. Parker, and D. R. Rolison, 2016 NRL Base Program Review—Surface Chemistry Branch, U. S. Naval Research Laboratory, 28 February 2016.

12. (INVITED AWARD ADDRESS) "Surmounting the Roadblocks to Rechargeable Zinc–Air Batteries by 3D Architectural Redesign of the Air-Breathing Cathode and Zn Anode." <u>E. S. Nelson</u>, J. F. Parker, P. A. DeSario, J. W. Long, D. R. Rolison and C. N. Chervin in the INOR award symposium on Frontiers in Undergraduate Research, 251st Meeting of the American Chemical Society, San Diego, CA, 13–17 March 2016.

13. (INVITED) "Architectural Design In 3D Physically Thwarts Dendrite Formation—With Zinc Now Rechargeable, Who Needs Lithium Batteries?" <u>D. R. Rolison</u>, J. F. Parker, C. N. Chervin, and J. W. Long, Briefing to NATO Parliamentary Assembly, U. S. Naval Research Laboratory, Washington, DC, 11 April 2016.

14.   (INVITED) "Architectural Design in 3D Physically Thwarts Dendrite Formation—With Zinc Now Rechargeable, Who Needs Lithium Batteries?" J. W. Long, J. F. Parker, C. N. Chervin, and D. R. Rolison, Briefing to Representatives of the Naval Acquisitions Development Program, U. S. Naval Research Laboratory, Washington, DC, 14 April 2016.

15. (INVITED) "Architectural Design In 3D Physically Thwarts Dendrite Formation—With Zinc Now Rechargeable, Who Needs Lithium Batteries?" J. W. Long, J. F. Parker, C. N. Chervin, and D. R. Rolison, Briefing to the Maverick Charm City Group, U. S. Naval Research Laboratory, Washington, DC, 20 April 2016.

16. (INVITED) "Next-Generation Rechargeable Zinc Batteries Based on Advanced 3D Electrode Designs." J. W. Long, C. N. Chervin, J. F. Parker, and D. R. Rolison, 47th Power Sources Conference, Orlando, FL, 13–16 June 2016.

17. (INVITED) "Enhancing Electrochemical Energy Storage on the Macroscale via Architectural Design on the Nanoscale." D. R. Rolison, National Institute of Standards & Technology, Gaithersburg, MD, 16 September 2016

18. (INVITED   PLENARY) "Designing   Catalytic   and   Energy-Relevant   Multifunctional Architectures." D. R. Rolison, 2016 SNO (Sustainable Nanotechnology Organization) Conference, 10–12 November 2016, Orlando, FL.

19. (INVITED) "3D Zn Sponge Anodes Enable Rechargeable Zinc-Based Alkaline Batteries." D. R. Rolison, J. F. Parker, and J. W. Long, Telebriefing to Drs Filippo Ronzani and Emanuele Instuli, Industrie De Nora S.p.A., 20 December 2016.

20. (INVITED) "3D Zn Sponge Anodes Enable High-Power Silver–3D Zinc-Based Alkaline Batteries." D. R. Rolison, J. F. Parker, and J. W. Long, Briefing to Mr. Mitchell Weinberg, Zennavision Partners, LLC, U. S. Naval Research Laboratory, 20 December 2016.

21. (INVITED) "Aerogels: An Architectural Guide to Advances in Energy." D. R. Rolison in Symposium NM3: Aerogels and Aerogel-Inspired Materials, *Spring Meeting of the Materials Research Society*, Phoenix, AZ, 17–21 April 2017.

22. (INVITED) "Rechargeable Nickel–3D Zinc Batteries: An Energy-Dense, Safer Alternative to Lithium-Ion." D. R. Rolison, J. F. Parker, J. W. Long, M. F. Burz, Call-in Press Conference, U. S. Naval Research Laboratory, Washington, DC, 27 April 2017.

23. (INVITED) "3D Zn Sponge Anodes Enable Rechargeable Zinc-Based Alkaline Batteries." J. W. Long, D. R. Rolison, and J. F. Parker, Briefing to RADM D. J. Hahn, U. S. Naval Research Laboratory, Washington, DC, 28 April 2017.

24. (INVITED) "3D Zn Sponge Anodes Enable High-Power Silver–3D Zinc-Based Alkaline Batteries." D. R. Rolison, J. F. Parker, and J. W. Long, Briefing to Mitchell Weinberg, Zennavision Partners, LLC and Paul Arena, Intellectual Property Network, U. S. Naval Research Laboratory, Washington, DC, 8 May 2017.

25. (INVITED) "Architecture as a Design Metaphor for Improving Multifunctional Activity." D. R. Rolison, J. F. Parker, J. W. Long, P. A. DeSario, and J. J. Pietron, Briefing to Drs. Filippo Ronzani and Emanuele Instuli, Industrie De Nora S. p. A., U. S. Naval Research Laboratory, Washington, DC, 16 May 2017.

26. (INVITED) "Safe, Rechargeable Zinc Batteries for DoN Applications." J. W. Long, J. F. Parker, and D. R. Rolison, OPNAV Briefing to Mr. David Cherry, NSWC-Carderock Detachment, U. S. Naval Research Laboratory, Washington, DC, 30 May 2017.

27. (INVITED) "Next-Generation Safe, Rechargeable Zinc Batteries ... Thanks to Zinc Architectures." D. R. Rolison, J. F. Parker, J. S. Ko, and J. W. Long, Advanced Automotive Battery Conference (AABC 2017), San Francisco, CA, 19–22 June 2017.

28. (INVITED) "Next-Generation Rechargeable Batteries Enabled by 3D Zinc Anodes." J. W. Long, J. F. Parker, and D. R. Rolison, Briefing to ONR Logistics Program, U. S. Office of Naval Research, Arlington, VA, 21 June 2017,

29. (INVITED) "3D Zn Sponge Anodes Enable Rechargeable Zinc-Based Alkaline Batteries." D. R. Rolison, J. F. Parker, and J. W. Long, Telebriefing to Dr. Ashok Sarawat, NEC Energy Solutions, Inc., 23 June 2017.

30. (INVITED) "Safe, Rechargeable Zinc Batteries for DoN Applications." J. W. Long, J. F. Parker, and D. R. Rolison, Briefing to Director Michael McClatchey, SEA 07D, and Ms. Amy Wing, PMS 394, U. S. Naval Research Laboratory, Washington, DC, 26 June 2017.

31. (INVITED) "Next-Generation Rechargeable Batteries Enabled by 3D Zinc Anodes." J. F. Parker, J. S. Ko, J. W. Long, and D. R. Rolison, Briefing to Michael Burz and George Mavko, EnZinc, Inc., U. S. Naval Research Laboratory, Washington, DC, 12 July 2017.

32. (INVITED) "Advanced 3D Electrode Designs for Safer Electrochemical Energy & Power." D. R. Rolison, J. F. Parker, and J. W. Long, Briefing to representatives from Stanley Black & Decker, U. S. Naval Research Laboratory, Washington, DC, 17 July 2017.

33. (INVITED) "Next-Generation Rechargeable Zinc Batteries as a Safe Alternative to Lithium-Ion." J. W. Long, D. R. Rolison, and J. F. Parker, Briefing to DASN Operational Energy and OPNAV N45, U. S. Naval Research Laboratory, Washington, DC, 14 August 2017.

34. (INVITED) "Next-Generation Rechargeable Zinc Batteries Enabled by 3D Zinc Anodes." <u>D. R. Rolison</u>, <u>J. F. Parker</u>, and <u>J. W. Long</u>, Briefing to representatives of Lockheed Martin Corp., U. S. Naval Research Laboratory, Washington, DC, 17 August 2017.

35. (INVITED) "Next-Generation Rechargeable Zinc Batteries as a Safe Alternative to Lithium-Ion." <u>J. F. Parker</u>, <u>D. R. Rolison</u>, and <u>J. W. Long</u>, Briefing to Drs Bruce Danly (DOR: NRL) and Richard Carlin (Office of Naval Research), U. S. Naval Research Laboratory, Washington, DC, 18 August 2017.

36. (INVITED) "Why Are We Leaving So Much Power & Energy on the Table?" <u>D. R. Rolison</u>, 10th Potters Lodge Meeting (PLM10), Blue Mountain Lake, NY, 6–10 September 2017

37. (INVITED) "Next-Generation Rechargeable Aqueous Batteries Enabled by 3D Zinc Anodes." <u>D. R. Rolison</u>, J. F. Parker, and J. W. Long, Briefing to the Defense Science Study Group (DSSG), DARPA, U. S. Naval Research Laboratory, Washington, DC, 14 September 2017.

38. (INVITED) "Effect of Ni:Fe Stoichiometry and Architectural Expression on the Bifunctional Activity of Nanoscale $Ni_yFe_{1-y}Ox$." <u>J. S. Ko</u>, J. W. Long, J. F. Parker, and D. R. Rolison in L09: Multi-Electron Redox Systems for Next Generation Batteries, 232nd Meeting of the Electrochemical Society, National Harbor, MD, 1–5 October 2017.

39. (INVITED) "Capabilities and Opportunities for Next-Generation Ag–3D Zn Batteries." <u>J. F. Parker</u>, J. S. Ko, J. W. Long, and D. R. Rolison in L09: Multi-Electron Redox Systems for Next Generation Batteries, 232nd Meeting of the Electrochemical Society, National Harbor, MD, 1–5 October 2017.

40. "Rechargeable Zn–Air Batteries Enabled By Zn Sponge Anodes and Bi(tri?)Functional Cathodes." <u>J. F. Parker</u>, J. S. Ko, C. N. Chervin, M. N. Vila, D. R. Rolison, and J. W. Long, in A05: Battery Materials: Beyond Lithium-Ion, 232nd Meeting of the Electrochemical Society, National Harbor, MD, 1–5 October 2017.

41. "From Designing and Characterizing Multifunctional Nanoarchitectures to Commercializing Zinc Sponge–Based Alkaline Batteries that Refuse to Launch Dendrites." <u>D. R. Rolison</u>, J. W. Long, and J. F. Parker in E03: Electrochemical Science and Engineering on the Path from Discovery to Product, 232nd Meeting of the Electrochemical Society, National Harbor, MD, 1–5 October 2017.

42. (INVITED) "Next-Generation Rechargeable Aqueous Batteries Enabled by 3D Zinc Anodes." <u>D. R. Rolison</u>, J. F. Parker, and J. W. Long, Briefing to RADM W. J. Galinis, PEO Ships, U. S. Naval Research Laboratory, Washington, DC, 1 November 2017.

43. (INVITED) "The Road to Safe, High-Performance Energy Storage Is Paved with Zinc." <u>J. F. Parker</u>, J. W. Long, D. R. Rolison, and J. S. Ko, Cambridge Innovation Institute's 8th Annual Battery Safety Meeting, Arlington, VA, 2–3 November 2017.

44. (INVITED) "Architectural Design in 3D Physically Thwarts Dendrite Formation—With Zinc Now Rechargeable, Who Needs Lithium Batteries?" <u>D. R. Rolison</u>, Dept of Materials Science & Engineering, North Carolina State University, Raleigh, NC, 17 November 2017.

45. (INVITED) "Architectural Design in 3D Physically Thwarts Dendrite Formation—With Zinc Now Rechargeable, Who Needs Lithium Batteries?" <u>D. R. Rolison</u>, Dept of Chemistry, University of Utah, Salt Lake City, UT, 8 December 2017.

46. (INVITED) "Zinc Sponges for Primary Alkaline Batteries." <u>D. R. Rolison</u>, <u>J. F. Parker</u>, and <u>J. W. Long</u>, Telebriefing to Drs. George Schimek, Weiwei Huang, Christina Hicks, and colleagues, Energizer Manufacturing, Inc., U. S. Naval Research Laboratory, Washington, DC, 9 January 2018.

47. (INVITED) "Next-Generation Rechargeable Batteries Enabled by 3D Zinc Anodes." <u>D. R. Rolison</u>, <u>J. F. Parker</u>, <u>J. W. Long</u>, and <u>M. F. Burz</u>, NRL/EnZinc Telebriefing to Drs. David Pappas, Ewa Ravenda, Dr. Steven Specht, and colleagues, Duracell, Inc., U.S. Naval Research Laboratory, Washington, DC, 26 January 2018.

48. (INVITED) "Architectural Design in 3D Physically Thwarts Dendrite Formation—With Zinc Batteries Now Rechargeable, What's Next?" <u>D. R. Rolison</u>, J. F. Parker, J. S. Ko, and J. W. Long, Gordon Research Conference on Batteries, Ventura, CA, 25 February–2 March 2018.

49. (INVITED) "Returning to Zinc to Meet the Challenges of Next-Generation Energy Storage." <u>J. F. Parker</u>, J. S. Ko, J. W. Long, and D. R. Rolison, 29th Annual Kavli Frontiers of Science Symposium, Irvine, CA, 15–17 February 2018.

50. (INVITED) "Dendrite-Free Rechargeable Zinc-Based Batteries: Solving a Chronic Impediment Through Architectural Design." <u>D. R. Rolison</u>, J. F. Parker, J. W. Long, and J. S. Ko in the Next-Generation Battery Research Track, International Battery Seminar, Fort Lauderdale, FL, 27–28 March 2018.

51. (INVITED) "Next-Generation Rechargeable Zinc Batteries Enabled by 3D Zinc Anodes." <u>J. W. Long</u>, J. F. Parker, and D. R. Rolison, Federal Laboratory Exchange Energy Storage Webinar, Washington, DC, 27 March 2018.

52. (INVITED) "Architectural Design in 3D Physically Thwarts Dendrite Formation and Enables Next-Generation Rechargeable Zinc Batteries as a Safer Alternative to Lithium-Ion." <u>D. R. Rolison</u>, J. F. Parker, J. S. Ko, and J. W. Long in Symposium EN14: Materials Science & Device Engineering for Safe & Long-Life Electrochemical Energy Storage, Spring Meeting of the Materials Research Society, Phoenix, AZ, 2–6 April 2018.

53. (AWARD ADDRESS) "Architectural Design, 1D Walls, 3D Plumbing, and Painting Blind en Route to Scalable Multifunctional Nanoarchitectures for Energy Storage." <u>D. R. Rolison</u>, William H. Nichols Medal Award Symposium, White Plains, NY, 13 April 2018.

54. (INVITED) "Architectural Design in 3D Physically Thwarts Dendrite Formation—With Zinc Now Rechargeable, Who Needs Lithium Batteries?" <u>D. R. Rolison</u>, Dept of Materials Science & Engineering, Drexel University, Philadelphia, PA, 25 April 2018.

55. (INVITED) "Architectural Design in 3D Physically Thwarts Dendrite Formation—With Zinc Now Rechargeable, Who Needs Lithium Batteries?" <u>D. R. Rolison</u>, Dept of Chemical & BioEngineering, University of California-Berkeley, Berkeley, CA, 2 May 2018.

56. "Rechargeable Zn–Air Batteries Enabled by Multifunctional Air Cathodes and Zn Sponge Anodes." <u>J. F. Parker</u>, J. S. Ko, D. R. Rolison, and J. W. Long, 48th Power Sources Conference, Denver, CO, 11–14 June 2018.

57. (INVITED KEYNOTE) "Effect of Stoichiometry and Architectural Expression on the Activity of Oxygen Reduction and Evolution Electrocatalysts." <u>D. R. Rolison</u>, J. S. Ko, C. N. Chervin, M. N. Vila, P. A. DeSario, J. F. Parker, and J.W. Long in the symposium on Sustainable Energy Conversion via Innovative Electrocatalysis & Photocatalysis, 256th Meeting of the American Chemical Society, Boston, MA, 19–23 August 2018 [18-1231-2878]

58. (INVITED) "Next-Generation, Rechargeable Zinc Batteries through 3D Electrode Design." <u>J. W. Long</u>, J. F. Parker, J. S. Ko, and D. R. Rolison, ENFL Symposium on Battery Technology: Vehicle to Grid, 256th Meeting of the American Chemical Society, Boston, MA, 19–23 August 2018 [18-1231-2515]

59. (INVITED) "Effect of Pore–Solid Architectural Expression on the Activity of Oxygen Reduction and Evolution Electrocatalysts." <u>D. R. Rolison</u>, J. S. Ko, C. N. Chervin, M. N. Vila, P. A. DeSario, J. F. Parker, and J.W. Long, 10th International Mesostructured Materials Symposium (IMMS-10), UCLA, Los Angeles, CA, 10–13 September 2018 [18-1231-3104]

60. (INVITED) "Redesign of Active Materials en Route to Safe, High-Performance Batteries and Supercapacitors that Use Aqueous Electrolytes." <u>J. W. Long</u>, J. F. Parker, M. B. Sassin, J. S. Ko, and D. R. Rolison, OUSD(R&E) Basic Research Office Forum, Office of Naval Research, Arlington, VA, 13 September 2018.

61. (INVITED) "(More) Uniform Control of Oxidative Dissolution, Complexation, and Electrodeposition Using 3D Wiring of Aperiodic Zinc Sponge Anodes in Rechargeable Alkaline Batteries." <u>J. W. Long</u>, J. S. Ko, A. B. Geltmacher, J. F. Parker, and D. R. Rolison, E04: Electroplating of Reactive Metals and Alloys for Energy Storage, 234th Meeting of the Electrochemical Society and SMEQ Joint International Meeting, Cancún, Mexico, 30 September–4 October 2018 [18-1231-2879]

62. (INVITED) "Update on Next-Generation Rechargeable Aqueous Batteries Enabled by 3D Zinc Anodes." <u>J. W. Long</u>, <u>J. F. Parker</u>, <u>B. J. Hopkins</u>, and <u>D. R. Rolison</u>, Teleseminar to Duracell R&D, Bethel, CT, 19 October 2018.

63. (INVITED) "Understanding Nickel–Zinc Batteries." <u>J. W. Long</u>, J. F. Parker, and D. R. Rolison, NATTBAT Workshop on Zinc Battery Technology in Stationary Energy Storage Applications, CUNY, New York, NY, 16 November 2018 [18-1231-4009]

64. (INVITED) "Dendrite-Free Rechargeable Zinc-Based Batteries: Solving a Chronic Impediment through Architectural Design." <u>D. R. Rolison</u>, J. S. Ko, J. F. Parker, A. B. Geltmacher, and J. W. Long in ET06: Advanced Materials and Chemistries for High-Energy and Safe Rechargeable Batteries, Fall Meeting of the Materials Research Society, Boston, MA, 25–30 November 2018.

65. (INVITED KEYNOTE) "Architectural Design in 3D Physically Thwarts Dendrite Formation— With Zinc Now Rechargeable, What's Next?" <u>D. R. Rolison</u>, J. F. Parker, J. S. Ko, B. J. Hopkins, C. N. Chervin, A. B. Geltmacher, and J. W. Long, Symposium on New Concepts, Materials, and Systems, International Battery Association (IBA2019), La Jolla, CA, 3–8 March 2019.

66. (INVITED) "Architectural Design in 3D Physically Thwarts Dendrite Formation—With Zinc Now Rechargeable, What's Next?" <u>D. R. Rolison</u>, J. F. Parker, J. S. Ko, B. J. Hopkins, C. N. Chervin, and J. W. Long, ENFL Symposium on Innovative Chemistry and Materials for Electrochemical Energy Storage, 257th Meeting of the American Chemical Society, Orlando, FL, 31 March–4 April 2019 [19-1231-0958]

67. "Bifunctional Cathode Configurations in Rechargeable Zn–Air Cells." <u>C. N. Chervin</u>, J. S. Ko, J. F. Parker, B. J. Hopkins, J. W. Long, and D. R. Rolison, ES09: Advanced Materials for the Water-Energy Nexus, Spring Meeting of the Materials Research Society, Phoenix, AZ, 22–26 April 2019.

68. (INVITED) "Architectural Design in 3D Physically Thwarts Dendrite Formation—With Zinc Now Rechargeable, What's Next?" <u>D. R. Rolison</u>, J. F. Parker, J. S. Ko, B. J. Hopkins, C. N. Chervin, and J. W. Long, ES09: Advanced Materials for the Water–Energy Nexus, Spring Meeting of the Materials Research Society, Phoenix, AZ, 22–26 April 2019.

69. (INVITED KEYNOTE) "Effect of Architecturally Expressed Electrodes and Catalysts on Energy Storage/Conversion in Aqueous Electrolytes." <u>D. R. Rolison</u>, J. F. Parker, J. S. Ko, B. J. Hopkins, C. N. Chervin, P. A. DeSario, M. B. Sassin, and J. W. Long, I05: Heterogeneous Functional Materials for Energy Conversion and Storage 2, 235th Meeting of the Electrochemical Society, Dallas, TX, 26–31 May 2019.

70. "Opportunities for 3D Zinc Anode Architectures in Aqueous Batteries." <u>D. R. Rolison</u>, J. S. Ko, B. J. Hopkins, J. F. Parker, C. N. Chervin, and J. W. Long, A05: Alternative Battery Chemistries and High-Power Devices, Electrochemical Conference on Energy and the Environment (ECEE 2019): Bioelectrochemistry and Energy Storage, Glasgow, Scotland, 21–26 July 2019.

71. (INVITED) "Alkaline Batteries with 3D Wired Zinc Architectured Anodes Are Now Rechargeable—What's Next?" D. R. Rolison, J. S. Ko, B. J. Hopkins, J. F. Parker, C. N. Chervin, and J. W. Long, Symposium on Women in Renewable Energy (WiRE), SPIE Optics and Photonics Meeting, San Diego, CA, 11–15 August 2019.

72. "Integrating Pseudocapacitive Function into Air-Cathodes with 3D-Wired Nanoscale MnOx: Enabling Pulse-Power for Zn–Air Batteries." C.N. Chervin, J.W. Long, M.B. Sassin, J.F. Parker, B.J. Hopkins, and D.R. Rolison, Fast Electrochemical Processes and Devices 3, 236th Meeting of The Electrochemical Society, Atlanta, GA, 13–17 October 2019.

73. "Manufacturing methods for large-format, rechargeable Zn-sponge electrodes." B.J. Hopkins, C.N. Chervin, J.F. Parker, J.W. Long, and D.R. Rolison, Advanced Manufacturing Methods for Energy Storage Devices 2, 236th Meeting of The Electrochemical Society, Atlanta, GA, 13–17 October 2019.